

University of Louisville

ThinkIR: The University of Louisville's Institutional Repository

Electronic Theses and Dissertations

12-2018

Restoring cholesterol homeostasis in familial hypercholesterolemia cell line model

Lubna Hindi
University of Louisville

Follow this and additional works at: <https://ir.library.louisville.edu/etd>



Part of the [Molecular, Cellular, and Tissue Engineering Commons](#)

Recommended Citation

Hindi, Lubna, "Restoring cholesterol homeostasis in familial hypercholesterolemia cell line model" (2018). *Electronic Theses and Dissertations*. Paper 3452.
Retrieved from <https://ir.library.louisville.edu/etd/3452>

This Master's Thesis is brought to you for free and open access by ThinkIR: The University of Louisville's Institutional Repository. It has been accepted for inclusion in Electronic Theses and Dissertations by an authorized administrator of ThinkIR: The University of Louisville's Institutional Repository. This title appears here courtesy of the author, who has retained all other copyrights. For more information, please contact thinkir@louisville.edu.

RESTORING CHOLESTEROL HOMEOSTASIS IN FAMILIAL
HYPERCHOLESTEROLEMIA CELL LINE MODEL

By

Lubna Hindi
B.S., University of Louisville, 2017

A Thesis
Submitted to the Faculty of the
University of Louisville
J.B. Speed School of Engineering
as Partial Fulfillment of the Requirements
for the Professional Degree

MASTER OF ENGINEERING

Department of Bioengineering

December 2018

RESTORING CHOLESTEROL HOMEOSTASIS IN FAMILIAL
HYPERCHOLESTEROLEMIA CELL LINE MODEL

Submitted by: _____
Lubna Hindi

A Thesis Approved On

(Date)

by the Following Reading and Examination Committee

Dr. Nolan L. Boyd, Thesis Co-Director

Dr. Patricia A. Soucy, Thesis Co-Director

Dr. Bradley B. Keller, Committee Member

Dr. Martin G. O'Toole, Committee Member

ACKNOWLEDGMENTS

Thank you to my mentor, Dr. Nolan Boyd, for his patience, guidance, laughs, and the opportunity to grow as a scientist while working in his lab. Thank you to my co-director, Dr. Patricia Soucy, for her extraordinary mentorship and advisement throughout this whole process. Thank you to my committee members, Dr. Brad Keller and Dr. Martin O'Toole, for their time and input on this project. Thank you to my lab mate, Linda Omer, for the mentorship she provided along with the sass and laughs. Thank you to Giuseppe Militello and Zhengzhi Xie for their help and input on this work.

Finally, thank you to my family, Musa, Sajedah, Samiha, Yousef, Mohammad, Balsam, Dabdoob, Mia, Fried Chicken, Eminem, and my amazing and inspiring mother. None of this would have been possible without your unconditional support and encouragement.

ABSTRACT

Familial hypercholesterolemia (FH) is an autosomal dominant disorder that results in elevated levels of low-density lipoprotein cholesterol (LDL-C). This increase in serum cholesterol level has been shown to result in premature coronary artery disease (CAD) with devastating symptoms from a young age. Today, the prevalence of heterozygous FH (HeFH) and homozygous FH (HoFH) is estimated to be 1 in 320 and 1 in 160,000 people, respectively. FH is referred to as an underdiagnosed disease due to the large number of mutations that continues to grow. These mutations often exist in one of or a combination of three genes: low-density lipoprotein receptor (LDLR), apolipoprotein B (APOB100), or proprotein convertase subtilin/kinase 9 (PCSK9) (S. Singh & Bittner, 2015). Mutations in the LDLR adapter protein 1 (LDLRAP1) were also identified as a less common cause of FH, the autosomal recessive variety, specifically. In treating the disease, patients are prescribed various treatment protocols aimed at reducing endogenous cholesterol synthesis, removal of excess cholesterol through extracorporeal machinery, and other medications aimed at upregulating the LDL receptors in the body. To this day, liver transplants remain as the only cure for FH.

FH-induced pluripotent stem cells (FH-iPSC) derived from HoFH skin fibroblasts were permanently corrected using CRISPR technology to insert the three missing base pairs and restore transport of the LDL receptor from the endoplasmic reticulum (ER) to the Golgi body. Hepatocytes are the cells primarily responsible for LDL-C uptake from the plasma, so we differentiated non-corrected familial hypercholesterolemia (NC) and CRISPR-corrected (C) iPSC to hepatocyte-like cells (HLC) to analyze restoration of cholesterol homeostasis. iPSC and HLC were treated with Rosuvastatin, excess sterols, or tunicamycin and collected for mRNA analysis and protein analysis of LDLR and ER stress markers. HLC were also treated with Rosuvastatin and

immunocytochemistry and the ThermoFisher Amplex Red Cholesterol Assay kit were used to analyze localization of LDLR within the cell and internalization of cholesterol, respectively.

Statin-treated NC-iPSC and HLC showed predominant expression of an immature LDLR protein that was not present in C-iPSC or HLC and this upregulation was not the result of regulation at the transcriptional level. The LDLR co-localized to ER resident-protein, Calnexin, in NC-HLC whereas the LDLR co-localized to the cell-membrane in the C-HLC. Upon correcting expression of the mature LDLR, cholesterol internalization increased overtime in C-HLC in contrast to a minimal amount internalized at the 24-hour mark in the NC-HLC. Lastly, statin-treated NC-iPSC and HLC were not observed to induce ER stress as represented by markers XBP1 and BiP.

TABLE OF CONTENTS

APPROVAL PAGE	ii
ACKNOWLEDGMENTS	iii
ABSTRACT	iv
LIST OF TABLES	vii
LIST OF FIGURES	viii
INTRODUCTION	1
Background	1
Previous Work	20
Objective	22
PROCEDURE	23
RESULTS	35
CONCLUSION	46
FUTURE WORK	50
APPENDIX	52
REFERENCES	53
VITA	58

LIST OF TABLES

Table 1 – Classes of LDLR mutations

Table 2 – Cell therapy categories

LIST OF FIGURES

Figure 1 – Small nodule present on the inner eye of the Mona Lisa

Figure 2 – LDLR diagram

Figure 3 - Cholesterol synthesis

Figure 4 – LDLR pathway

Figure 5 – Pathways of the unfolded protein response

Figure 6 – Differentiation timeline

Figure 7 – Chamber slide set-up for ICC

Figure 8 – LDLR protein expression in iPSC and HLC

Figure 9 – LDLR transcripts in iPSC and HLC

Figure 10 – Localization of the LDLR in HLC

Figure 11 – Cholesterol internalization in HLC

Figure 12 – DiI LDL internalization in HLC

Figure 13 – HMG-CoA reductase activity in HLC

Figure 14 – BiP expression in iPSC and HLC

Figure 15 – XBP1 expression in iPSC and HLC

I. INTRODUCTION

A. Background

Familial hypercholesterolemia (FH) is an autosomal dominant disorder that results in elevated levels of low-density lipoprotein cholesterol (LDL-C) (Bouhairie & Goldberg, 2015). Historically, the prevalence of heterozygous FH (HeFH) and homozygous FH (HoFH) was estimated to be 1 in 500 and 1 in one million, respectively, but more recent studies suggest a prevalence closer to 1 in 320 and 1 in 160,000 people (de Ferranti et al., 2016; Sjouke et al., 2015). These numbers might even be higher, but accurate estimates of FH prevalence are difficult to obtain as there is no independent code assigned to this disease by the World Health Organization (WHO) (Nordestgaard et al., 2013). Additionally, most countries lack a national FH registry and no uniform criteria for FH exists (Akiyamen et al., 2017). It is also referred to as an underdiagnosed disease due to the large number of mutations that continues to grow (Soutar & Naoumova, 2007). These mutations often exist in one of or a combination of three genes: low-density lipoprotein receptor (LDLR), apolipoprotein B (APOB100), or proprotein convertase subtilin/kinase 9 (PCSK9) (S. Singh & Bittner, 2015). Mutations in the LDLR adapter protein 1 (LDLRAP1) were also identified as a less common cause of FH, the autosomal recessive variety, specifically (Harada-Shiba et al., 1992).

1. Clinical Discovery

Familial hypercholesterolemia was first described by Norwegian doctor, Carl Müller, in the late 1930's after studying 17 families in Oslo where 68 of 76 members presented with both some form of xanthoma and heart disease (Müller, 1939). Xanthomas, depositions of yellow

cholesterol-rich material composed of lipids, were first described by Addison and Gull in 1851, but the discovery of associated increased levels of cholesterol wouldn't be made until 1920 by Chauffard and Burns (Burns, 1920). Today, the presence of xanthoma accounts for one out of three criteria, at least two of which need to be met, in order to diagnose FH (Harada-Shiba et al., 2018). Xanthomas have become such a common indicator of FH, that historians are now describing the Mona Lisa painting by Leonardo da Vinci as the first case of FH due to the presence of a small yellowish nodule at the inner end of her left eyelid as indicated in **Figure 1** (Ose, 2008). da Vinci was known for his work in atherosclerotic disease so it is possible that his inclusion of this nodule was intentional (Keele, 1951). In the 1960's, Dr. Khachadurian categorized hypercholesterolemia into three categories – homozygous FH, heterozygous dominant FH, and heterozygous recessive FH – after analyzing a number of Lebanese families and describing the codominant inheritance of the disease (Khachadurian, 1964).

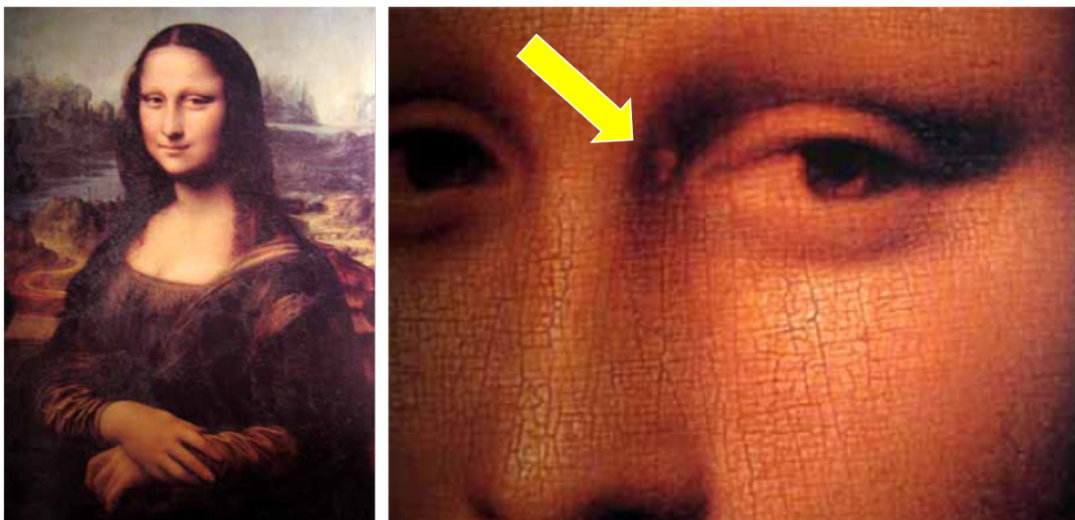


Figure 1 – A small yellowish nodule present on the inner eyelid of the Mona Lisa by Leonardo da Vinci (Kuzaj, Kuhn, Faust, Knabbe, & Hendig, 2014)

2. The Low-Density Lipoprotein Receptor

The low-density lipoprotein receptors (LDLRs or LDL receptors) in hepatocytes act as the primary method of cholesterol removal from plasma through receptor-mediated endocytosis. The LDL receptor is a transmembrane protein with 5 domains as represented in **Figure 2** below: LDLR repeat domain, EGF repeat domain, O-linked glycosylation domain, transmembrane domain, and cytoplasmic domain (Jain, Jain, Kesharwani, & Jain, 2013; Lagor & Millar, 2009). The LDLR repeat domain is responsible for ligand binding, specifically apolipoprotein B100 (ApoB100) on LDL and ApoE. The epidermal growth factor (EGF) repeat domain consists of three repeated sequences. The first of these two domains are linked to the third by a sub-domain of 6 short amino acid repeats to form a six-bladed β -propeller. This β -propeller interacts with the LDLR repeat domain and contributes to ligand release from the receptor after internalization has occurred. The O-linked sugars on the O-linked glycosylation domain are thought to prevent proteolytic cleavage of the extracellular domain while it sits on the plasma membrane. Mutations in this domain have shown no effect on ligand binding. The transmembrane domain anchors the LDLR to the plasma membrane. Finally, the cytoplasmic domain contains a glycine that is required for proper sorting of the receptor to the plasma membrane after synthesis of the receptor.

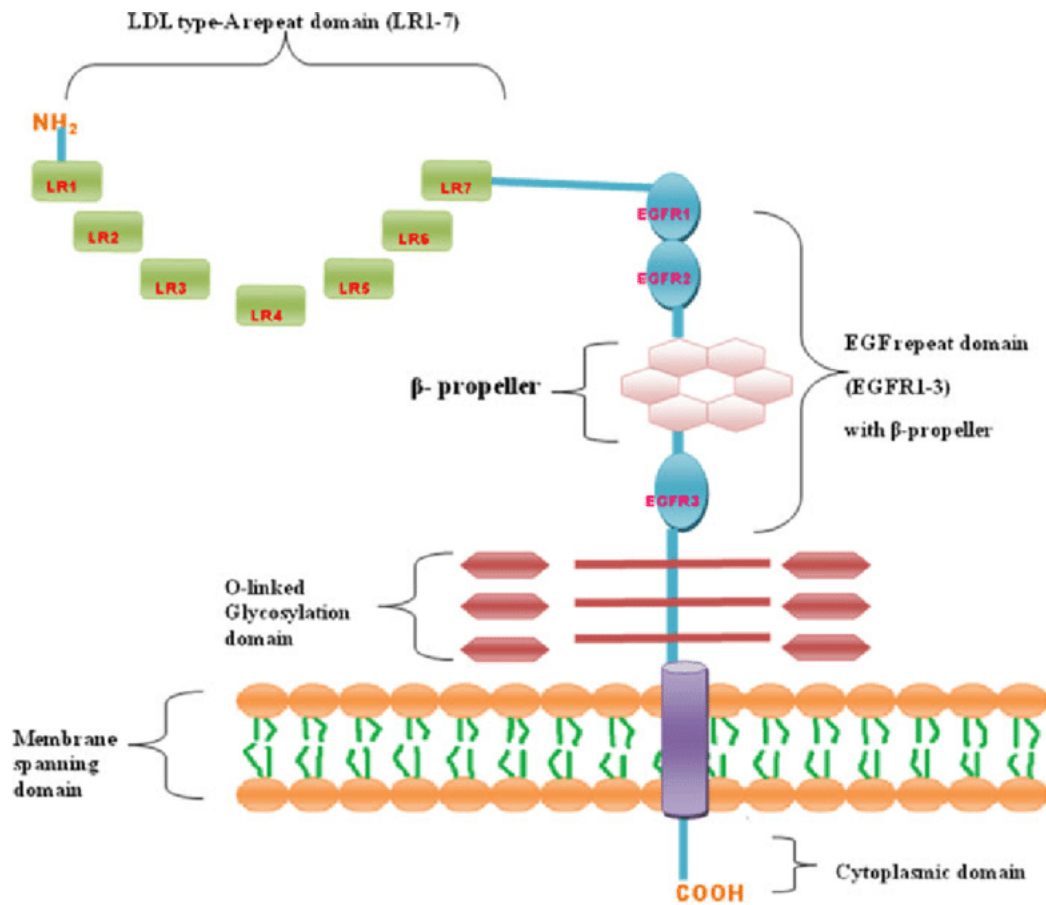


Figure 2 – The five domains of the low-density lipoprotein (LDL) receptor (Jain et al., 2013)

3. Sources of Cholesterol

FH is a disorder characterized by disruption in LDL-C metabolism and so it is important to briefly review this pathway and that of cholesterol synthesis. All of the cholesterol present in the human body arises from one of two sources: ingestion of cholesterol-containing foods or de novo synthesis within cells (Cerqueira et al., 2016).

Dietary Cholesterol. The human body absorbs more than 95% of ingested fatty acid and monoacylglycerols (Pan & Hussain, 2012). Once ingested, dietary cholesterol is formed into

micelles by bile salt activity and presented to mucosal enterocytes in the intestine (Lu, Lee, & Patel, 2001). Upon absorption into enterocytes in the jejunum of the small intestine, free cholesterol and fatty acids are re-esterified by acyl-coenzyme A:cholesterol acyl-transferase and packaged into chylomicrons with triglycerides, phospholipids, and apolipoprotein B-48 (Dawson & Rudel, 1999). Chylomicrons transport lipids absorbed in the intestine to adipose, cardiac, and muscle tissue where lipoprotein lipase (LPL) hydrolyzes the triglyceride component (Dash, Xiao, Morgantini, & Lewis, 2015). Chylomicrons are secreted from the basolateral aspect of the enterocytes into the lymphatic channels and reaches the liver where it can be packaged into lipoproteins and secreted into the plasma or secreted into bile (Crawford et al., 1997).

Endogenous Cholesterol Synthesis. There are approximately 45 steps that take place in cholesterol biosynthesis as summarized in **Figure 3**. The first of which begins with the enzyme thiolase catalyzing the reaction to form acetoacetyl-CoA from two acetyl-coenzyme A (acetyl-CoA) molecules. Next, 3-hydroxy-3-methylglutaryl-CoA (HMG-CoA) synthase catalyzes the reaction to form HMG-CoA from acetoacetyl-CoA and another molecule of acetyl-CoA. Next, HMG-CoA reductase, the rate-limiting enzyme of the mevalonate pathway, catalyzes the NADP-dependent synthesis of mevalonate from HMG-CoA. Inhibiting HMG-CoA reductase is a common target for pharmaceutical drugs for FH in order to decrease the amount of endogenously produced cholesterol. Once mevalonate is synthesized, it is converted into two activated isoprenes, isopentanyl 5-pyrophosphate and dimethylallyl pyrophosphate, before a series of condensations of activated isoprenes take place to form a 30-carbon molecule called squalene, the biochemical precursor of all steroids. It has to be converted to lanosterol, which is then transformed into cholesterol after a number of reactions. Cholesterol that exceeds the needs of the cell is transported through the blood as very low-density lipoprotein (vLDL) (Berg, 2002). These particles are either

taken up by the liver for processing or converted into low-density lipoprotein (LDL). LDL delivers cholesterol throughout the body for use in cell membranes, hormone production, Vitamin D production, and bile acid synthesis (Cortes et al., 2014).

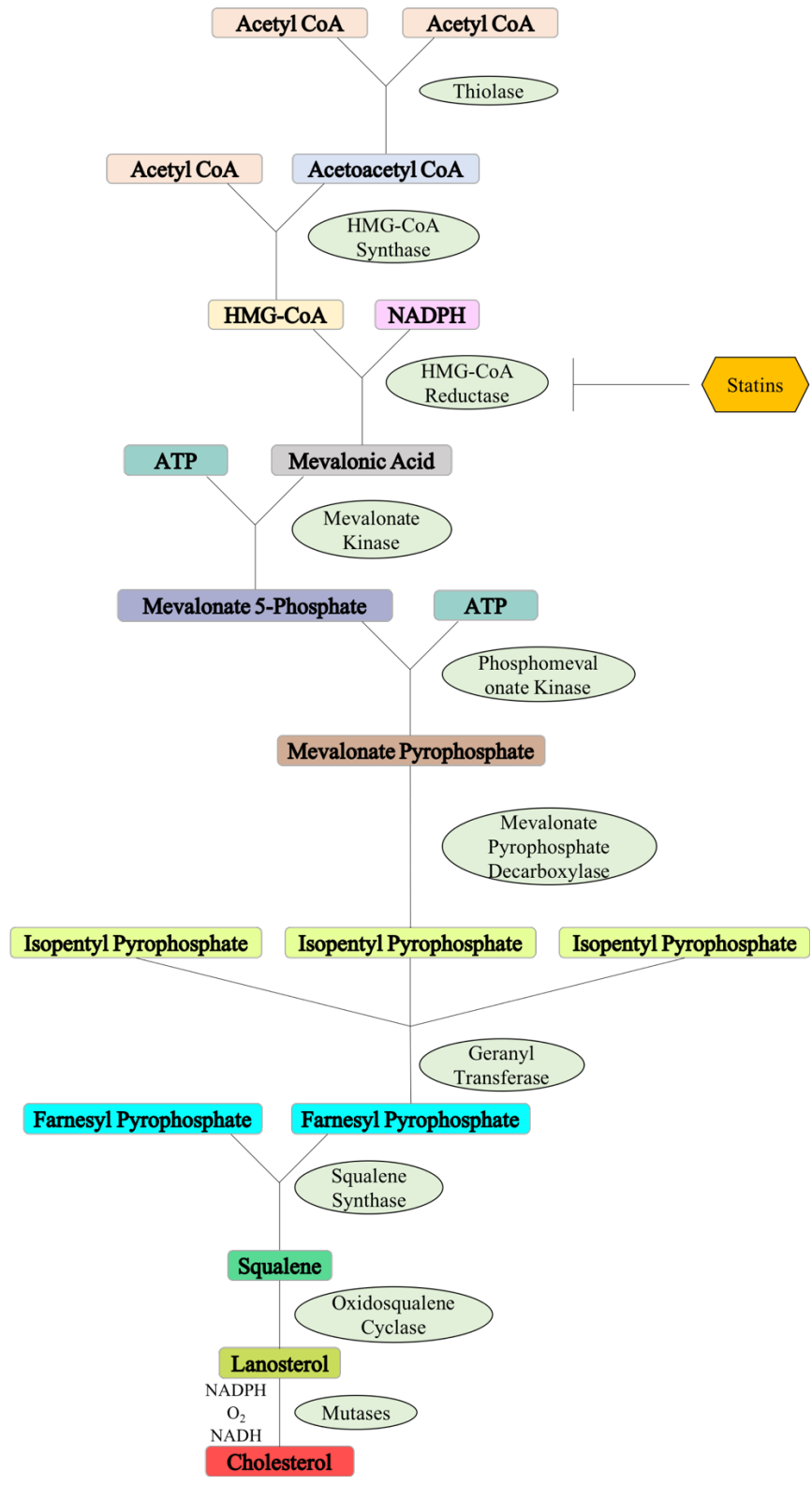


Figure 3 – Cholesterol synthesis

4. Receptor-Mediated Endocytosis

In receptor-mediated endocytosis, a specific receptor on the cell surface binds to the extracellular molecule of interest before it undergoes endocytosis and becomes a transport vesicle for further processing within the cell (Lodish, 2000). LDL, as mentioned earlier, has a large protein called ApoB100. ApoB100 is what is recognized by the LDL receptor in order to bind the LDL particle (Brown & Goldstein, 1979). Once the LDL particle is bound, the LDL receptor clusters into a clathrin-coated pit that encloses the LDL receptor and begins to form a coated endocytic vesicle. Next, this vesicle detaches from the membrane to carry the LDL into the cell where it's taken into a lysosome. Once inside the lysosome, the LDL receptor detaches from the LDL particle and is recycled back to the cell surface. The LDL particle remains inside the lysosome and is degraded. When LDL receptors are no longer needed, PCSK9 binds to the EGF-A repeat domain on the LDLR to mark it for degradation by lysosomes. Mutations in the APOB100, LDLR, or PCSK9 genes will disrupt this pathway and can result in increased levels of LDL-C. This process is summarized in **Figure 4**.

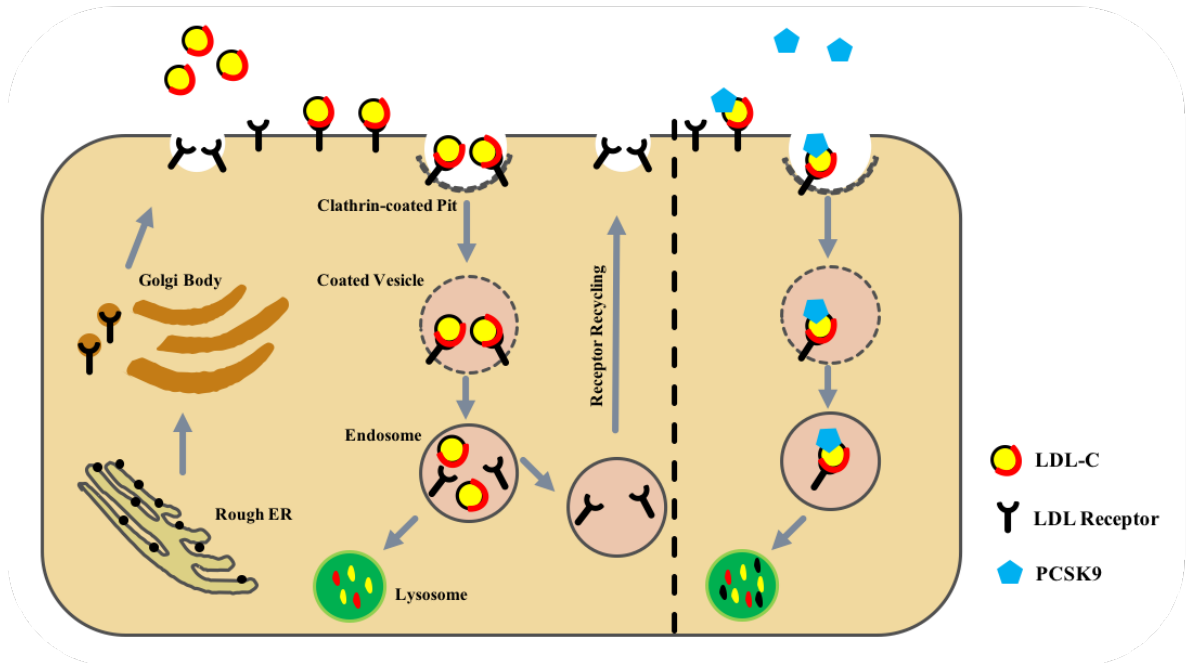


Figure 4 – LDLR pathway

5. Mutations in Cholesterol Metabolism

With respect to FH, mutations in the PCSK9 gene are gain-of-function mutations that increase the degradation of the LDL receptor and in turn decrease LDL-C uptake, leaving it to circulate within the body (Sharifi, Futema, Nair, & Humphries, 2017). Pharmaceutical drugs that inhibit PCSK9 synthesis are also common in certain types of FH with the goal of decreasing LDLR degradation by PCSK9 in order to increase LDL-C uptake. Loss-of-function mutations within the PCSK9 gene also exist, but do not lead to FH as they decrease the degradation of LDL receptors which in turn decreases the amount of LDL-C in the body and results in a 28% lower risk of coronary heart disease (Benn, Nordestgaard, Grande, Schnohr, & Tybjaerg-Hansen, 2010). Mutations in the APOB100 gene that cause FH are due to missense mutations that result in a ligand-defective ApoB100 protein. This renders the LDL-C particle unable to bind to the LDL

receptor and in turn continues to circulate in the blood (Myant, 1993). Mutations in the LDLR, the most common FH-causing mutations, are loss-of-function mutations. As of 2017, there are more than 2,600 mutations in the LDLR gene that cause FH, all of which can be categorized into one of five classes of mutations as summarized in **Table 1** (H H Hobbs, D W Russell, M S Brown, & Goldstein, 1990).

TABLE 1
CLASSES OF LDLR MUTATIONS

Classification	Mutation
Class I	LDLR is not synthesized
Class II	LDLR not properly transported from ER to Golgi apparatus
Class III	LDLR unable to properly bind LDL on cell surface
Class IV	LDLR bound to LDL unable to be internalized
Class V	LDLR is not recycled to cell surface

Class I mutations result in no synthesis of the LDL receptor. Class II mutations disrupt the transport of the receptor due to improper folding that prevents them from meeting the criteria needed to exit the ER and travel to the Golgi body for further modification. The mutation in the cells of this study is characterized as a Class II mutation. Class III mutations affect the binding of the LDL to the receptor. Class IV mutations prevent the internalization of the receptor once it has bound an LDL particle. Finally, Class V mutations prevent receptors from being recycled to the plasma membrane and leave them to be degraded along with the LDL particle in the lysosome upon initial internalization.

Heterozygous FH (HeFH) is caused by inheriting one mutated allele and one normal allele. This is the most common type of FH and results in LDL-C levels in the 350-550 mg/dL range, a 200% increase of normal LDL-C levels that range from 100-190 mg/dL (Pejic, 2014). Homozygous FH (HoFH), the more devastating type, is caused by inheriting two mutated alleles. This results in LDL-C levels in the 650-1,000 mg/dL range, a 500% increase over normal levels. Within these categories exist sub-types that further characterize the type of FH a person has. In true homozygous FH, the same mutation is observed in both alleles. This type is less common than compound heterozygous FH, different mutations are observed in each allele of the same gene, or double heterozygous FH, mutations in two different genes affect the LDLR function (Cuchel et al., 2014). Elevated levels of LDL-C, as early as the fetus, as a result of these mutations result in accelerated levels of cholesterol deposition and development of atherosclerosis (Brown & Goldstein, 1986; Buja, Kovanen, & Bilheimer, 1979). The development of atherosclerosis will often lead to premature coronary heart disease (CHD) in men and women by ages 50 and 60, respectively (Hopkins, Toth, Ballantyne, & Rader, 2011). It is estimated that 5% of myocardial infarctions (MIs) in patients <60 years and 20% of MIs in patients <45 years are a result of FH. HoFH patients, untreated, will develop overt atherosclerosis before the age of 20 and typically don't survive past age 30 (Goldstein & Brown, 2001).

6. Endoplasmic Reticulum Stress

The endoplasmic reticulum (ER) is the organelle where protein folding occurs for proteins destined for intracellular organelles and the cell surface (Kaufman, 2004). There are a number of cell signaling pathways that regulate mRNA translation and prevent accumulation of unfolded protein by decreasing the load, increasing the folding capacity, and increasing the degradation of

misfolded proteins. Before exiting the ER to be transported elsewhere, proteins are sorted to determine if a protein is properly folded and is able to leave the ER. Otherwise retention signals are sent to prohibit the protein from exiting and eventually degrading the misfolded protein (Ellgaard & Helenius, 2003). This retention in the ER also extends the amount of time a protein is exposed to the folding machinery and increases the chance of correct and proper folding. The protein concentration in the ER lumen is relatively high, 100 mg/mL, requiring protein chaperones to facilitate the folding process to prevent aggregation that could cause ER stress and activate the unfolded protein response. These protein chaperones and folding sensors include BiP, calnexin, calreticulin, glucose-regulated protein (GRP)94, thiol-disulphide oxidoreductases protein disulphide isomerase (PDI), and ERp57 ("Calnexin, calreticulin and the folding of glycoproteins," 1997; Fra, Fagioli, Finazzi, Sitia, & Alberini, 1993; Hellman, Vanhove, Lejeune, Stevens, & Hendershot, 1999).

Three branches of the UPR have been identified and work in parallel to increase folding capacity, decrease folding load, or degrade accumulated protein to allow the cell to restore homeostasis or apoptose ((Ron & Walter, 2007). The three signal transducers are activating transcription factor 6 (ATF6), double-stranded RNA-activated protein kinase (PKR)-like ER kinase (PERK), and inositol requiring enzyme 1 (IRE1). Their pathways have been summarized in **Figure 5** and will be discussed here briefly. The first transducer, ATF6, is a transcription factor

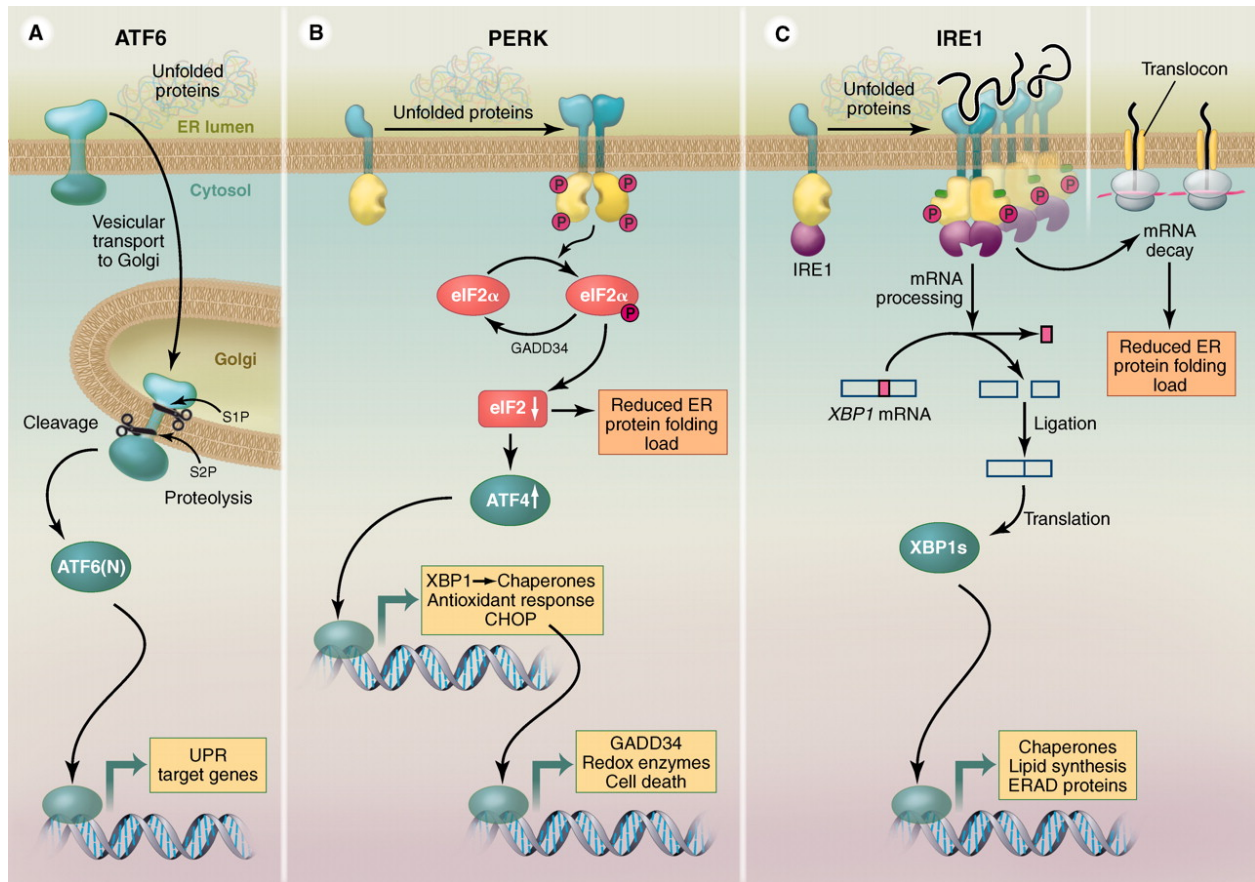


Figure 5 – Three pathways of the unfolded protein response (Ron & Walter, 2007).

that is packaged into vesicles and transported to the Golgi apparatus upon protein accumulation (Schindler & Schekman, 2009). ATF6 encounters two proteases that remove the luminal domain to allow the liberated N-terminal cytosolic fragment to move to the nucleus and activate UPR target genes including BiP. ATF6 increases the folding capacity of the ER. The second transducer, PERK, oligomerizes and phosphorylates itself when sensing ER stress. It also phosphorylates the ubiquitous translation initiation factor eIF2 α which inactivates eIF2 and inhibits mRNA translation. Some mRNAs that contain short open reading frames are preferentially translated and encode the ATF4 transcription factor and induces its translation. ATF4 targets CCAAT-enhancer-

binding protein homologous protein (CHOP) and growth arrest and DNA damage-inducible 34 (GADD34). CHOP controls genes involved in apoptosis and so the PERK pathway also contributes to signaling cell-death. PERK reduces the flux of protein entering the ER to reduce folding load. Lastly, the IRE1 pathway uses mRNA splicing to transmit the UPR signal. It becomes activated by conformational changes after lateral IRE1 oligomerization in the ER membrane. Upon activation, IRE1 cleaves the mRNA encoding the UPR-specific transcription factor, X-box binding protein 1 (XBP1) and the severed exons are then ligated and result in spliced XBP1. IRE1 pathway is also responsible for reducing the folding load in the ER.

Little research has been published about ER stress specific to HoFH. Jorgensen et al. showed the molecular chaperone BiP co-immunoprecipitates with both wild type and two different mutant LDL receptors in lysates from human liver cells that overexpressed wild type or mutant LDL receptors. They concluded that BiP was co-immunoprecipitated with the mutant receptors five times more than the wild type receptors suggesting that BiP is involved in the retention mutant LDL receptors in the ER (Jorgensen et al., 2000). In Sorensen et al., Chinese hamster ovary (CHO) cells were transfected with mutant LDLR and showed increase in the activity of IRE1 and PERK concluding that retention of the mutant LDLR in the ER induces ER stress.

7. Current Treatment

In patients with FH, the primary goal of treatment is the management and prevention of further atherosclerotic coronary artery disease through control of cholesterol levels as there continues to be no cure beyond liver transplantation for FH. These treatments include lifestyle changes, drugs that target PCSK9, HMG-CoA reductase, or dietary cholesterol absorption, bile-acid sequestrants, lipid apheresis, liver transplants, and gene therapies (Lambert et al., 2014).

Lifestyle changes include avoiding smoking, participating in regular physical activity, and following dietary recommendations. Patients are told to follow a fat-reduced diet which provides 25-35% of total caloric intake, saturated fats less than 7% of total caloric intake, less than 200 mg of cholesterol per day, increased intake of monosaturated and polyunsaturated fats and fiber, and plant sterols, 2 mg daily. Statins are a competitive inhibitor of HMG-CoA reductase and will work to block cholesterol synthesis in the liver and in turn decrease LDL production. They are the first line of pharmacologic agents used in treating FH and are recommended for use to reduce LDL-C by at least 50% from baseline. Even with aggressive statin therapy, the majority of FH patients don't reach more than a 50% reduction in LDL-C and are recommended to incorporate cholesterol absorbing inhibitors as well. Cholesterol absorption inhibitors block the absorption of dietary cholesterol and delivery of intestinal cholesterol to the liver. This leads to an up-regulation in LDL receptors on hepatocytes and increased uptake of LDL-C. This treatment was found to decrease LDL-C levels by an additional 15% when used in conjunction with statin treatments (Stein et al., 2007).

Bile acid sequestrants (BASs) have also been shown to lower LDL-C levels. Bile acids are digestive surfactants that promote the absorption of lipids by acting as emulsifiers (Staels & Fonseca, 2009). When a meal is ingested, the gallbladder contracts and releases bile acids into the intestinal lumen to aid in this ingestion. Enterohepatic circulation allows for 95% of bile acids to be reabsorbed and transported back into the liver. Bile acid sequestrants work by binding negatively charged bile acids in the intestinal lumen to divert the bile acids from enterohepatic cycling and instead into the feces for excretion (Insull, 2006). This prevents bile acids from cycling and aiding in the absorption of LDL-C. BASs were originally the first treatment for FH, but are now used as a 2nd or 3rd line of treatment after statins. Another recommended treatment for FH is

through inhibiting PCSK9. PCSK9, as mentioned earlier, is responsible for premature LDL receptor degradation. Inhibiting PCSK9 would result in increased levels of LDL receptors and increased uptake in LDL-C. PCSK9 inhibitors are injectable monoclonal antibodies that bind to PCSK9 to prevent their degradation of LDLRs. The ability of anti-PCSK9 therapies to significantly lower LDL-C levels have enabled the frequency of other treatments, such as lipid apheresis to be markedly reduced (Ogura, 2018). Lipid apheresis removes circulating LDL by removing blood from a vein, separating it into cellular and plasma components, removing LDL, and returning the blood to the patient. There are methods that don't involve separation of plasma and cells, direct lipoprotein adsorption, where polyacrylamide beads with pores that only allow certain particles, such as LDL, to enter and be removed. Lipid apheresis imposes a great burden on the patient in the form of high costs per treatment, high frequency of treatments needed, and long time to complete each treatment, 3-5 hours. Many patients drop out of therapy as a result of the physical or financial problems related to it. In HeFH patients, these treatments often work well in order to achieve relatively, more normal LDL-C levels, at least a 50% reduction. In HoFH patients, these treatments are aimed at lowering cholesterol levels in order to avoid a liver transplant.

Liver transplants remain the only option for HoFH patients that don't respond to pharmacological agents. They replace the dysfunctional hepatic LDL receptors to allow the patient to reach near normal levels of LDL-C through normal metabolism. The long-term outcomes are unknown due to a number of factors. There are limited organ donors, need for life-long immunosuppressive therapy, and a high risk in post-operational outcomes. However, recent data has shown the five-year survival rate after liver transplants to near 90% in pediatric patients

(Kusters et al., 2010). With liver transplants as the only cure for HoFH patients, gene therapies have been explored as an alternate treatment option.

The goal of gene therapy is to deliver a functional LDLR transgene to the liver. In 1995, Grossman et al. performed the first gene therapy clinical trial in HoFH patients with little success (Grossman et al., 1995). An ex vivo approach was used to transfer replication-deficient human LDLR-expressing retroviruses into the liver. The patients first underwent resection of the hepatic left-lateral segment, their hepatocytes were harvested, transduced ex vivo using the retrovirus vector, and then infused back into the donors through the portal vein. Only few transduced hepatocytes were observed and the reduction in LDL-C levels varied between 6-25%. These findings confirmed the feasibility of LDLR gene therapy in humans, but required further work in order to be successfully implemented. Recently, a recombinant adeno-associated virus (AAV) vector has entered clinical testing as the most developed form of gene therapy (Ajufo & Cuchel, 2016). AAV is a replication-defective, non-pathogenic parvovirus that retains its DNA in the host cell nucleus in a circular episomal form allowing for stable gene expression in post-mitotic tissue. The first AAV vector developed achieved efficient gene transfer and stable hepatocyte transduction, but expressed poor liver tropism in humans. Multiple different AAV vectors have been developed that differ in tropism and immunogenicity to allow for broader use in gene therapy. Most recently, AAV8 was used for liver-directed gene therapy in HoFH and compared well in relation to the earlier vectors AAV2 and AAV7. AAV8 was associated with more efficient gene transfer, hepatocyte transduction, and more complete lipid correction.

8. Cell Therapy

Cell therapy has emerged as a plausible alternative to many treatments used for liver diseases. Cells serve as an effective and favorable treatment due to their ability to work together to perform complex functions and have behavior that can be specifically engineered based on the desired need (Fischbach, Bluestone, & Lim, 2013). Cell therapy can be categorized based on a number of groups – method of delivery, cell line, cell source, and cell in vivo half-life – all of which are summarized in **Table 2** (Bhatia, Underhill, Zaret, & Fox, 2014; Culme-Seymour, Davie, Brindley, Edwards-Parton, & Mason, 2012; Nicolas, Wang, & Nyberg, 2016). The use of induced pluripotent stem cells (iPSC) has emerged as an attractive branch of cell therapy. In 2006, Takahashi and Yamanaka reprogrammed somatic cells into iPSC using four reprogramming factors, Octamer binding transcription factor-4 (Oct4), Sex determining region Y – box 2 (Sox2), Kruppel Like Factor-4 (Klf4), and c-MYC (Takahashi & Yamanaka, 2006). They were demonstrated to be both self-renewing and able to differentiate like embryonic stem cells (ESC) and could provide an alternative to ESC to overcome ethical concerns.

Since their discovery, iPSC have been used in a number of applications including disease modeling, regenerative medicine, and drug discovery and cytotoxicity tests (V. K. Singh, Kalsan, Kumar, Saini, & Chandra, 2015). iPSC technology offers a number of advantages. iPSC are similar in their abilities to ESC and can be generated without using fertilized embryos, in turn overcoming ethical concerns associated with the use of ESC. They also present reduced chances of immunorejection. By using patient-derived cells and reprogramming them to iPSC before differentiation to another type of cell, the chances of immunorejection are reduced. This was also shown by Guha et al. who showed no evidence of increased T cell proliferation or an antigen-specific secondary immune response after transplanting iPSC derived embryonic bodies or tissue-

specific cells (Guha, Morgan, Mostoslavsky, Rodrigues, & Boyd, 2013). iPSC also provide a canvas for testing toxicity and therapeutic effect of newly developed drugs.

TABLE 2
CELL THERAPY CATEGORIES

Method of Delivery	
Cell Transplantation	Injection of whole cells
Bioartificial Organs	Whole cells in extracorporeal devices
Cell Line	
Primary Cell	Mature parenchymal cells
Stem Cells	Tissue-derived stem cells
Cell Source	
Allogenic	Human donor
Autologous	Self donor
Xenogeneic	Animal donor
Cell in vivo Half-Life	
Transient dosing	Days or weeks
Permanent implantation	Years

B. Previous Work

The aim of this study was to characterize the LDL receptor in CRISPR-corrected HLC derived from skin fibroblasts of HoFH patients. Our lab has previously shown the ability to restore LDL receptor-mediated endocytosis in HoFH-iPSC in Ramakrishnan et. al (Ramakrishnan et al., 2015). NC-iPSC were generated from FH fibroblasts and differentiated towards a hepatic lineage through a five-stage process. At the end of the fifth stage, almost 90% of cells were expression alpha fetoprotein (AFP), a major plasma protein produced by the yolk sac and fetal liver during development, and albumin, a protein made by the liver (Ramakrishnan et al., 2015). FH-iPSC were transfected with a pEHZ-LDLR-LDLR plasmid containing a wild-type LDLR and differentiated into mesenchymal cells. Upon treatment with excess sterols, cells showed little internalization of 1,1'-dioctadecyl-3,3,3',3'-tetramethyl-indocarbocyanine perchlorate (DiI-LDL), but a 2-fold increase in internalization with statin treatment.

In Omer et al., 3040 induced pluripotent stem cells (iPSC) were corrected using CRISPR (Omer et al., 2017). The parental GM03040 skin fibroblasts were reprogrammed to 3040-iPSC using a synthetic messenger RNA cocktail containing octamer-binding transcription factor 4 (OCT4), sex determining region Y-box (SOX2), Kruppel-like factor 4 (KLF4), c-mycproto-oncogene (C-MYC), and Lin-28 homolog A (LIN-28). The mutation of this specific HoFH patient was a Class II mutation due to a 3 base pair deletion (ACC) on exon 4 of the LDLR sequence. This mutation resulted in little to no LDL receptor-mediated LDL uptake due to misfolding of the LDLR protein. In order to correct the mutation, CRISPR was used to insert the missing 3 base pairs. The 3040-iPSC were transfected with Cas9 nickase (Cas9n) modified to incorporate green fluorescent protein (GFP), single-guide RNA 1 plasmids (sgRNA1) containing a red fluorescent protein (RFP), and single-stranded oligodeoxynucleotide (ssODN) and cells were sorted for dual-positive

expression (GFP and RFP) for further cell culture. Correction was also confirmed by restriction fragment length polymorphism (RFLP) by using the novel XmnI restriction site that was introduced with the donor repair template. Sanger sequencing was also used in order to confirm the presence of the previously-deleted 3 base pairs.

The corrected 3040-iPSC, non-corrected 3040-iPSC, and human embryonic stem cells (H1) were differentiated to hepatocyte-like cells (HLC) and treated with lovastatin, excess sterols, and low-density lipoprotein labeled with DiI-LDL to observe the effect of the correction. As expected, the lovastatin treatment resulted in induction of the LDLR in all three cells lines, but was primarily present in its immature form in the non-corrected 3040-iPSC with little mature protein present. The corrected 3040-iPSC expressed predominantly mature LDLR protein which further confirmed the correction had occurred and responded normally to statin treatment. The excess sterol treatment resulted in a down-regulation of LDLR expression across all cell lines suggesting regain of function of the LDLR in the corrected cells. DiI-LDL treatment was used to visualize the internalization of LDL. DiI-LDL depends on receptor-mediated endocytosis in order to be internalized into the cell, but it is important to note here that after a sufficient period of time, it can be internalized by the cell through non-receptor mediated pathways such as pinocytosis. The internalization of DiI-LDL by the corrected 3040-iPSC was similar to that of the control H1 cells whereas there was very little to no internalization by the non-corrected cells. Following this work, there still remained a number of questions regarding the cholesterol metabolism in the corrected cells and especially in the differentiated hepatocyte-like cells.

C. Objective

We hypothesized that a Class II LDLR mutation disrupts cholesterol homeostasis and induces ER stress and will be alleviated by correction of the LDLR. We aimed to determine the level of restoration of cholesterol metabolism and homeostasis in FH Class II mutant patient-derived cells after CRISPR correction. This was achieved by looking at key steps of cholesterol metabolism including the expression of the mature LDL receptor, the internalization of exogenously-introduced LDL, and HMG-CoA reductase activity.

II. PROCEDURE

A. Differentiation of Induced Pluripotent Stem Cells (iPSC) to Hepatocyte-Like Cells (HLC)

A protocol adapted from Hay et al. was used to differentiate induced pluripotent stem cells (iPSC) to hepatocyte-like cells (HLC) (Hay, Fletcher, et al., 2008; Hay, Zhao, et al., 2008). Familial hypercholesterolemia cells (NC) iPSC, CRISPR-corrected familial hypercholesterolemia (C) iPSC, and human embryonic stem cells (H1) (WiCell, Madison, WI) were cultured on hESC-Qualified Matrigel coated 35 mm tissue culture plates (BD Bioscience, San Jose, CA) in mTeSR1 (STEMCELL Technologies, Vancouver, Canada) in an incubator maintained at 5% CO₂ and 37°C. Upon reaching 70% confluency, cells were passaged using Versene (Thermo Fisher, Waltham, Ma) with 10 mM Rock inhibitor (Selleck Chemical, Houston, TX) into appropriately-sized tissue culture dishes as required by each experiment and allowed to grow. Differentiation commenced upon cells reaching 40% confluency and was performed as follows.

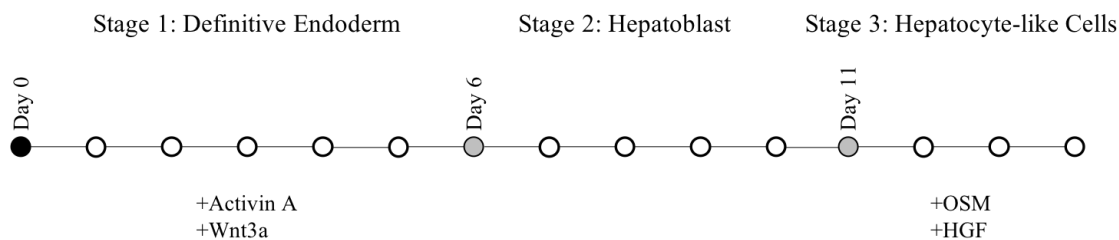


Figure 6 – Differentiation timeline

Cells were first differentiated to definitive endoderm in stage one. Stage one lasted five days and required daily media changes with fresh additions of Activin A [100 ng/mL] (Peprotech, Rocky Hill, NJ) and Wnt3a [50 ng/mL] (R&D Systems, Minneapolis, MN) in RPMI 1640 media (Invitrogen, Waltham, MA) with 1X B27 (Invitrogen). After five days of stage one, cells were

switched to stage two media requiring media changes every 48 hours for five days for the hepatoblast stage. Stage two media consisted of knockout Dulbecco's modified Eagle's medium (KO-DMEM) media (Invitrogen) supplemented with 20% knock-out serum replacement (Invitrogen), 0.5X GlutaMAX (Invitrogen), 1X nonessential amino acids (NEAA) (Invitrogen), 0.1 mM 2-mercaptoethanol (Thermo Fisher), and 1% (v/v) dimethyl sulfoxide (DMSO) (Sigma-Aldrich, St. Louis, MO). Finally, stage three, hepatocyte-like cell stage, required media changes every 48 hours for a maximum of 11 days. Stage three media consisted of HepatoZYME media (Invitrogen) supplemented with 0.5X GlutaMAX, 10 μ M Hydrocortisone-21 (Sigma-Aldrich), and hepatocyte growth factor (HGF) [10 ng/mL] (Peprotech) and Oncostatin M (OSM) [20 ng/mL] (Peprotech) added fresh.

B. LDLR Protein Expression in Statin-Treated iPSC and HLC

1. Cell Treatment

Non-corrected, corrected, and H1 iPSC or HLC were treated overnight with 5 μ M Rosuvastatin (EMD Millipore, Burlington, MA) or excess sterols (10 μ g/mL cholesterol and 5 μ g/mL 25-Hydroxycholesterol) (Sigma-Aldrich) in 5% lipoprotein-deficient serum media (LPDS) (Alfa Aesar, Tewksbury, MA). Control cells were treated with DMSO overnight. iPSC were used in experiments in order to look at how these cells might be affected by statin treatment as a way to replicate conditions experienced by pregnant women prescribed statins. HLC were used in experiments in order to look at how our correction affected cells differentiated to a mature hepatocyte-like stage. As described earlier, statins are an HMG-CoA Reductase inhibitor, the rate-limiting enzyme in cholesterol synthesis, and should result in upregulation of the LDLR in order to obtain cholesterol from an external source, the cell culture media in this case. Excess

sterols were used as a control to determine the functionality of our cells. Excess sterols are internalized by the cell through non-receptor mediated pathways and, as a result, downregulate the LDLR because the cholesterol needs of the cell have been met.

2. Cell Collection

Cells were washed twice with ice-cold phosphate buffered saline containing magnesium and calcium (PBS +/+) then scraped and collected in additional ice-cold PBS +/+. Collected samples were centrifuged (200 x g, 4 minutes) and pellets were resuspended in RIPA lysis buffer (Thermo Fisher), containing [1:100] protease and phosphatase inhibitor cocktail (Thermo Fisher), and lysed overnight at 4°C. The next day, cell lysates were centrifuged (13,000 x g, 10 minutes) and supernatants were transferred to new tubes to measure protein concentration using DC Protein Assay (Bio-Rad).

C. LDLR mRNA Expression in Statin-Treated iPSC and HLC

1. Cell Treatment

Non-corrected, corrected, and H1 iPSC or HLC were treated overnight with 5 µM Rosuvastatin or excess sterols in 5% lipoprotein-deficient serum media (LPDS) (Alfa Aesar, Tewksbury, MA). Control cells were treated with DMSO overnight.

2. Cell Collection and Sample Preparation

Cells were lysed using 150 µL of RLT Buffer (Qiagen, Valencia, CA) with 0.1% β-mercaptoethanol. Lysates were purified with QIAshredder and RNeasy kits (Qiagen) per kit instructions. RNA was quantified with a NanoDrop One Spectrophotometer (Thermo Fisher). Next, cDNA was synthesized using 1 µg RNA with SuperScript IV reverse transcriptase (Invitrogen) in a 20 µL volume. Finally, qPCR was performed using Fast SYBR Green Master

Mix (Thermo Fisher) with appropriate primers for the LDLR (Integrated DNA Technologies) as listed in the Appendix. Reactions were run on the StepOnePlus Real-Time PCR System (Thermo Fisher).

D. Localizing LDLR in HLC

1. Cell Treatment

Non-corrected and corrected HLC were plates in 4 wells of a 4-well chamber slide and differentiated as described above. Following differentiation, cells were treated with Rosuvastatin in LPDS overnight before preparing for imaging.

2. Preparation for Imaging

Cells were fixed with 2% paraformaldehyde (PFA) in PBS (10 minutes, 24°C) after. Next, cells were permeabilized with 0.05% Triton X-100/PBS (10 minutes, 24°C) (Sigma Aldrich) and washed with PBS. Cells were then blocked with 5% normal donkey serum/PBS (Jackson ImmunoResearch) for 1 hour before blocking with an avidin/biotin blocking kit (Vector Laboratories). Primary antibodies, calnexin (EMD Millipore, Billerica, MA) and biotinlated-wheat germ agglutinin (Vector Laboratories), were diluted in 5% donkey serum/PBS and incubated on cells overnight at 4°C. Secondary antibodies were also diluted (1:1000) in 5% donkey serum/PBS and added to the cells (2 hours, 24°C) before washing and mounting with VECTASHIELD Antifade Mounting Medium with DAPI. Slides were imaged with Olympus BX61W1 confocal microscope with Fluoview (FV10-ASW 4.1, Olympus) and analyzed with AMIRA software (Thermofisher). A list of antibodies used is available in the appendix.

3. Quantifying Colocalization

Fluoview (FB10-ASW 4.1) was used to analyze colocalization by using the colocalization tool under the processing tab to quantify overlap between selected channels and provide a visual representation of the overlap. To quantify images using the software, load the image and click on the “Processing” tab in the toolbar at the top of the page and select “Colocalization”. In the command window that appears, choose “Series” to analyze the full stack. Under the “Axis” options, choose the channels of interest for quantification (e.g. LDLR and Calnexin, LDLR and WGA). Under “Annotated Methods” select “Threshold” to provide a threshold value, above which the overlap will be considered. A value of 500 was used to begin when setting up with IgG controls, after the numbers given by the IgG control images were used as threshold values for the remaining images. Reselect the channels under “Axis” to update the statistics then click on “Statistics” located in the bottom corner of the command window. This provided values of overlap between channels. The overlap data provided a number representing the colocalization of a pixel from each channel throughout the entire stack. This also provided an image with the overlap between two channels pseudo colored to default white, we changed it to yellow for better visualization.

E. Cholesterol Internalization in HLC – Amplex Red Kit

1. Cell Treatment

Non-corrected and corrected cells were plated on 35 mm tissue culture dishes and differentiated until day one of stage three, as described above. On day two and three of stage three, media was replaced with lipoprotein-deficient serum (LPDS) media supplemented with 5 μ M Rosuvastatin and cells were incubated overnight. The following day, cells were treated with LPDS media supplemented with 5 μ M Rosuvastatin and 10 mM methyl- β -cyclodextrin (Sigma-Aldrich) for 45 minutes. Timepoint zero was collected after this treatment and the remaining culture dishes

were treated with LPDS media supplemented with 5 μ M Rosuvastatin and 10 μ g/mL unlabeled low-density lipoprotein (LDL). Cells were collected at six and 24 hours.

2. Cell Collection

Cells were collected by incubating in TrypLE Express (Thermo Fisher) for five minutes then gently scraped and transferred to 15 mL tubes and centrifuged (200 \times g, 4 minutes). The pellet was resuspended in a 200 μ L chloroform/methanol (2:1 v/v) mixture, vortexed, and centrifuged (14,000 \times g, 5 minutes) to allow separation into three layers. A micropipette was used to carefully discard the top layer. Next, a micropipette was used to gently push past the middle layer (a thin membrane) and transfer the bottom layer to new microcentrifuge tubes. These microcentrifuge tubes were dried using a vacuum for 30 minutes using a Savant SpeedVac Vacuum. The dried lipids were resuspended in 1X reaction buffer from the Amplex Red Cholesterol Assay Kit (Thermo Fisher). The middle layer was resuspended in RIPA lysis buffer and lysed overnight at 4°C. Cell lysates were centrifuged the next day (13,000 \times g, 10 minutes) and supernatants were transferred to new microcentrifuge tubes and used for protein analysis using DC protein assay (Bio-Rad).

3. Lipid Analysis and Normalization

Collected lipid content was analyzed using the Thermo Fisher Amplex Red Cholesterol Assay Kit per the instructions. Briefly, a 5.17 mM cholesterol reference was diluted in 1X reaction buffer to create a standard curve ranging from 0 to 20 μ M. The lipids collected from the cells, see section D.2 above, were pipetted in triplicates in a 96-well plate. A working solution was made by mixing Amplex Red reagent, HRP, cholesterol oxidase, cholesterol esterase, and 1X reaction buffer (concentrations as indicated by the kit instructions). Reaction samples were analyzed with an excitation of 560 nm and emission detection at 590 nm in a spectrophotometer. Lipid content

was normalized to total protein level as measured by the DC protein assay (Bio-Rad). Briefly, a standard curve was made using 1 mg/mL bovine serum albumin (BSA) and 0.9% NaCl solution as outlined in the table below.

TABLE 3
BSA STANDARD CURVE

Standard Tube Final [C] (μg)	BSA (μL)	NaCl (μL)
0.0 (blank)	0.0	50.0
1.0	5.0	45.0
2.5	12.5	37.5
5.0	25.0	25.0
7.5	37.5	12.5

Each standard was mixed with RIPA lysis buffer at a 1:1 ratio. 10 μL of sample was transferred to a new labeled microcentrifuge tube and 10 μL of NaCl solution was added. Standards and samples were pipetted in triplicates into a 96-well plate. Reagent A' was made by adding 20 μL of Protein Assay Reagent S to 980 μL Protein Assay Reagent A and vortex-mixed. 25 μL of Reagent A' was added to each well followed by 200 μL of Protein Assay Reagent B before incubating the plate at room-temperature for 5 minutes, protected from light. Finally, the plate was read at a wavelength of 750 nm in a spectrophotometer.

F. Cholesterol Internalization in HLC – Immunocytochemistry

1. Cell Treatment

Non-corrected and corrected cells were plated in 3 wells of a 4-well chamber slide and differentiated to day one of stage three. The next day, one well from each cell line was treated with 5 μ M Rosuvastatin in LPDS for 24 hours while the remaining two wells from each cell line stayed in stage three media. The following day, the well treated with Rosuvastatin was treated with 10 μ g/mL DiI-LDL (Alfa Aesar) and 5 μ M Rosuvastatin in LPDS for 24 hours. The remaining two wells from each cell line were treated with 5 μ M Rosuvastatin in LPDS for 24 hours. On the third day of treatment, with six hours remaining in the 24-hour period from the first well, 10 μ g/mL DiI-LDL and 5 μ M Rosuvastatin was added to the six hour well and the last well was left unchanged. The experiment was stopped when the first well reached 24 hours in DiI-LDL and Rosuvastatin incubation. Cells were continuously treated with Rosuvastatin as a way to upregulate the LDLR to maximize internalization of the DiI-LDL that was added in the cell culture media.

	t=24h	t=6h	t=0h
Label	Day 1: +RS	Day 1: No Change	Day 1: No Change
	Day 2: +DiI LDL +RS	Day 2: +RS	Day 2: +RS
	Day 3: No change	Day 3: +DiI LDL + RS	Day 3: No Change

Figure 7 – Chamber slide set-up for immunocytochemistry

2. Preparation for Imaging

Media was aspirated from all wells and replaced with 1X PBS ++ for three washes. After the last wash, cells were fixed with 2% PFA (Electron Microscopy Sciences, Hatfield, PA) for 10 minutes at room temperature. Cells were again quickly washed with 1X PBS ++ before adding

VECTASHIELD Antifade Mounting Media with DAPI (Vector Laboratories, Burlingame, CA) and securing a glass cover on top. Cells were imaged at 20X magnification using Olympus 1X81 fluorescence microscope (Center Valley, PA).

G. HMG-CoA Reductase Activity in HLC

1. Cell Treatment

Non-corrected and corrected cells were plated on 60 mm tissue culture dishes and differentiation began as described above upon reaching 75% confluency. Cells were differentiated to day one of stage three with treatment beginning the following day. Stage three media was replaced with LPDS and cells were incubated overnight. The following day, one dish from each cell line was collected as timepoint zero and the remaining dish from each cell line was treated with 10 µg/mL LDL in LPDS and incubated overnight and collected the following day.

2. Cell Collection

Cell collection and analysis protocol was adapted from Kuzaj et al (Kuzaj et al., 2014). Cells were washed twice with ice-cold PBS ++ then scraped and collected in additional ice-cold PBS ++. Collected samples were centrifuged (3000 x g, 5 minutes) at 4°C and the pellets were resuspended in 120 µL lysis buffer (137.6 mM NaCl, 50 mM Tris/HCl, 8.7% Glycerin, 0.5 mM EDTA, 1% Protease Inhibitor, and 1% NP-40). Lysates were frozen for 1 hour at -80°C and clarified by centrifugation (8000 x g, 10 minutes) at 4°C. Supernatants were transferred to new tubes and a 10 µL aliquot was used to perform a DC protein assay (Bio-Rad).

3. Sample Preparation

50 µg total protein/sample were transferred to new microcentrifuge tubes and Q.S.'d to 100 µL with enzyme reaction buffer (100 mM Potassium Phosphate Buffer, 0.1 mM EDTA, 50 mM KCl, 10 mM DTT, 2.5 mM NADPH, 15 mM Glucose-6-phosphate, and 1 unit of Glucose-6-phosphate dehydrogenase). Next, 50 µL of 200 µM HMG-CoA substrate in enzyme reaction buffer was added to reach a final volume of 150 µL. Samples were incubated at 37°C for 30 minutes after which the reaction was stopped with the addition of 20 µL 6 M HCl. 300 µL of acetonitrile containing 10 µg/mL mevalonolactone-4,4,5,5,6,6,6-d₇ (MVL-D₇) was added and samples were vortexed for 5 seconds then centrifuged (13,000 x g, 10 minutes) at 4°C. Supernatants were stored at -80°C.

4. Preparation for UPLC-MS/MS System

Samples were thawed and evaporated in a vacuum for 1.5 hours. Residues were dissolved in 50 µL HPLC-grade water/methanol/acetonitrile containing 0.5 M HCl (1:1:1 v/v) then vortex mixed for 10 seconds. Samples were centrifuged (13,000 x g, 10 minutes) and supernatants were transferred to autosampler vessels. 1 µL was injected into the ultra-performance liquid chromatography tandem mass spectrometry (UPLC-MS/MS) system.

5. Sample Protein Analysis

Samples were analyzed using western blot. 10 µg total protein/sample were loaded into 4-15% Mini-PROTEAN TGX Precast Protein Gels (Bio-Rad) and separated in 1X running buffer (10X Tris/Glycine/SDS buffer diluted in Milli-Q water) for 40 minutes at 200 V at room temperature. Gels were transferred onto methanol-activated PVDF membrane (Bio-Rad) in 1X transfer buffer at 100 V for 70 minutes at 4°C. Membranes were blocked in 3% non-fat milk in phosphate buffered saline with Tween 20 (PBST) and incubated in primary antibody overnight at

4°C (1:100 anti-HMG-CoA (Sigma-Aldrich) in PBS +/- or 1:1000 anti- β -actin (Santa Cruz Biotechnology, Dallas, TX) in 3% non-fat milk in PBST. The following day, membranes were washed three times for five minutes in 1X PBST then incubated in secondary antibody for one hour at room temperature (1:5000 anti-mouse IgG HRP-linked (Cell Signaling, Danvers, MA) in 3% non-fat milk in PBST. Afterward, membranes were again washed three times for five minutes in 1X PBST then developed with Clarity Max Western ECL Blotting Substrate (Bio-Rad) and imaged on the Bio-Rad Imager. A table of antibodies used is available in the Appendix.

H. ER Stress in iPSC and HLC

1. Cell Treatment

Non-corrected, corrected, and H1 iPSC or HLC were treated overnight with 5 μ M Rosuvastatin excess sterols (10 μ g/mL cholesterol and 5 μ g/mL 25-Hydroxycholesterol) (Sigma-Aldrich), or 5 μ g/mL tunicamycin (4 hours) (Invitrogen) in 5% LPDS (Alfa Aesar, Tewksbury, MA). Tunicamycin is a chemical activator of the unfolded protein response and acted as a positive control to verify that this pathway is in fact inducible in our cells. Control cells were treated with DMSO overnight.

2. Sample Collection and Analysis

Experiments were conducted and collected for mRNA or protein and analyzed as described previously but with markers for BiP and XPB1. Polymerase chain reaction (PCR) was carried out for spliced-XBP1 and XBP1 expression with PCR Supermix (Invitrogen). 10 μ L of amplicons were added to 2 μ L 6X Loading Buffer (Invitrogen) and run at 80 V for 60 minutes

using a 2% agarose gel (Bio-Rad). Gels were imaged using ChemiDoc MP Imaging System (Bio-Rad, Hercules, CA).

I. Statistical Analysis

Experiments were conducted with a sample size of $n=3$ and data was analyzed using one-way ANOVA with a post-hoc using Sidak's multiple comparison test in GraphPad Prism 8 and expressed as mean \pm SEM. Differences between control and treated samples were considered statistically significant at $p < 0.05$.

III. RESULTS

A. Rosuvastatin Upregulates LDLR Protein Levels and mRNA Transcripts in Non-Corrected and Corrected Cells

Non-corrected, corrected, and H1 iPSC or HLC were treated with Rosuvastatin or excess sterols in LPDS to analyze expression of LDLR protein and transcript levels in order to determine if the increase total LDLR protein observed earlier was a result of regulation at the transcriptional level. Excess sterols act independently of the LDLR and will enter the cell via non-receptor-mediated pathways, increasing the cholesterol content regardless of LDLR functionality. Rosuvastatin is an HMG-CoA Reductase inhibitor that will inhibit endogenous cholesterol synthesis. **Figure 8a and Figure 8b** show a significant upregulation in the expression of the immature LDLR protein in non-corrected iPSC and HLC that isn't present in the corrected or H1 cells indicating that the CRISPR correction mediated the mutation present in the non-corrected iPSC and HLC. For quantification, both immature, when present, and mature bands were used to quantify total LDLR protein levels.

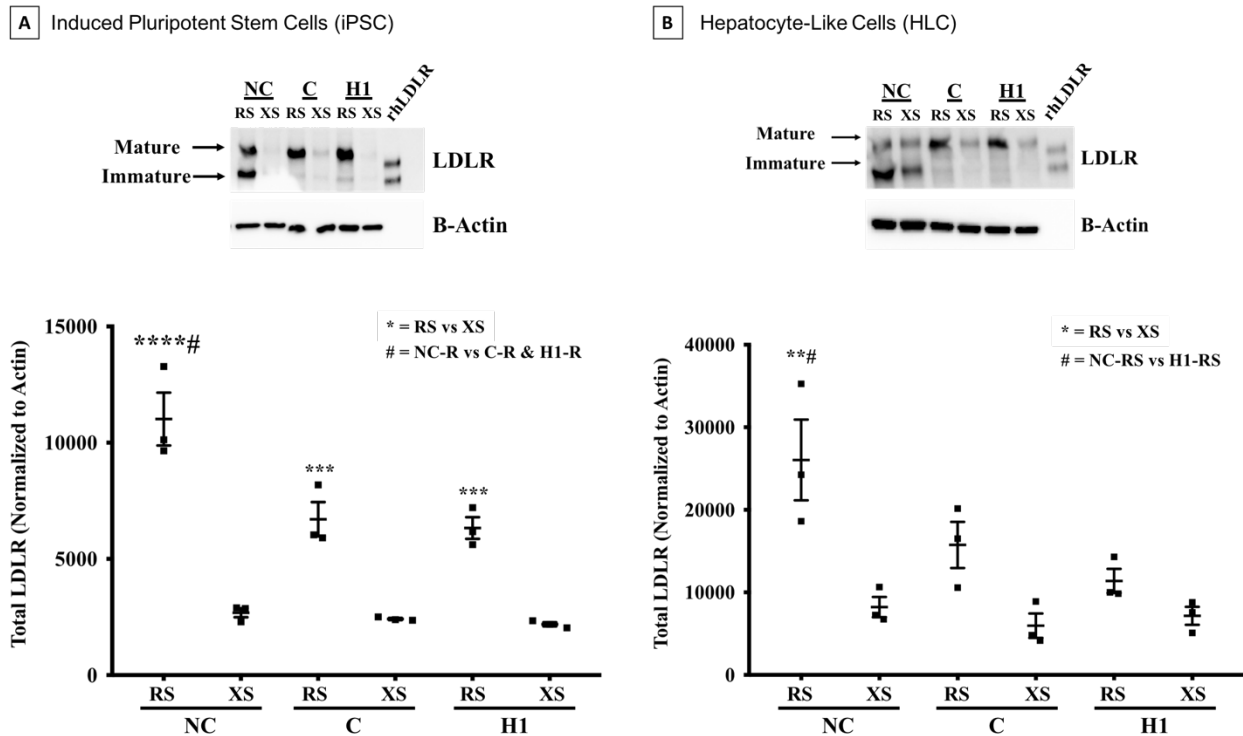


Figure 8 – LDLR protein expression in (A) iPSC and (B) HLC treated with Rosuvastatin (RS) or excess sterols (XS). *** $p < .001$, # $p < 0.05$.

Next, we looked at LDLR transcript levels to determine if the upregulation in immature LDLR in the non-corrected cells was the result of transcriptional regulation in the LDLR. qPCR analysis was conducted on iPSC and HLC treated with Rosuvastatin and excess sterols. **Figure 9a** and **Figure 9b** show no significant difference across cell lines in the LDLR transcript levels. The statistical significance displayed represents the difference between treatments within each cell line. This indicates that the Rosuvastatin, as expected, upregulated LDLR transcript levels in NC, C, and H1 iPSC and HLC, but there was no statistically significant difference in the increase between each cell suggesting the increase seen at the protein level is not a result of an increase at the transcriptional level.

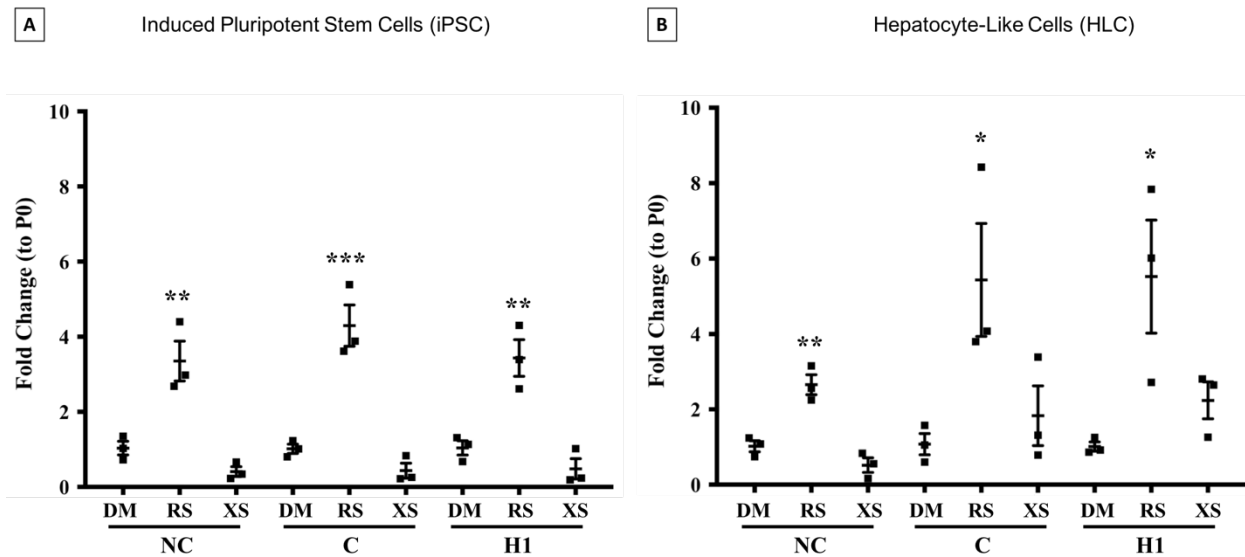


Figure 9 – LDLR transcript levels in (A) iPSC and (B) HLC treated with DMSO (DM), Rosuvastatin (RS), or excess sterols (XS). * $p < 0.05$, ** $p < 0.01$, *** $p < 0.001$.

B. LDLR Co-Localizes in ER in Non-Corrected HLC

Because we observed expression of majority immature LDL protein in the non-corrected cells, we looked at where the LDLR localized in the non-corrected HLC after Rosuvastatin treatment. As mentioned earlier, Calnexin is present in the ER and acts to retain misfolded proteins as one of its functions. Wheat germ agglutinin (WGA) binds to N-acetylglucosamine found in the plasma membrane and has been shown to bind to the hepatocyte cell membranes. HLC were treated with Rosuvastatin in LPDS overnight and confocal microscopy was used to determine localization of the LDLR protein. **Figure 10a** further confirms the upregulation of LDLR in Rosuvastatin-treated corrected and non-corrected HLC. We also included the images of the secondary control, labeled IgG, to show non-specific binding of the antibodies we used. **Figure 10b** presents the overlap of LDLR with calnexin or WGA where the overlap between the two channels is pseudo-colored yellow. This overlap was quantified and presented in **Figure**

10c. In the NC-HLC, we observed a significantly greater amount of LDLR overlap with calnexin when compared to LDLR overlap with WGA indicating a retention of the immature LDLR in the endoplasmic reticulum rather than its mature expression at the plasma membrane.

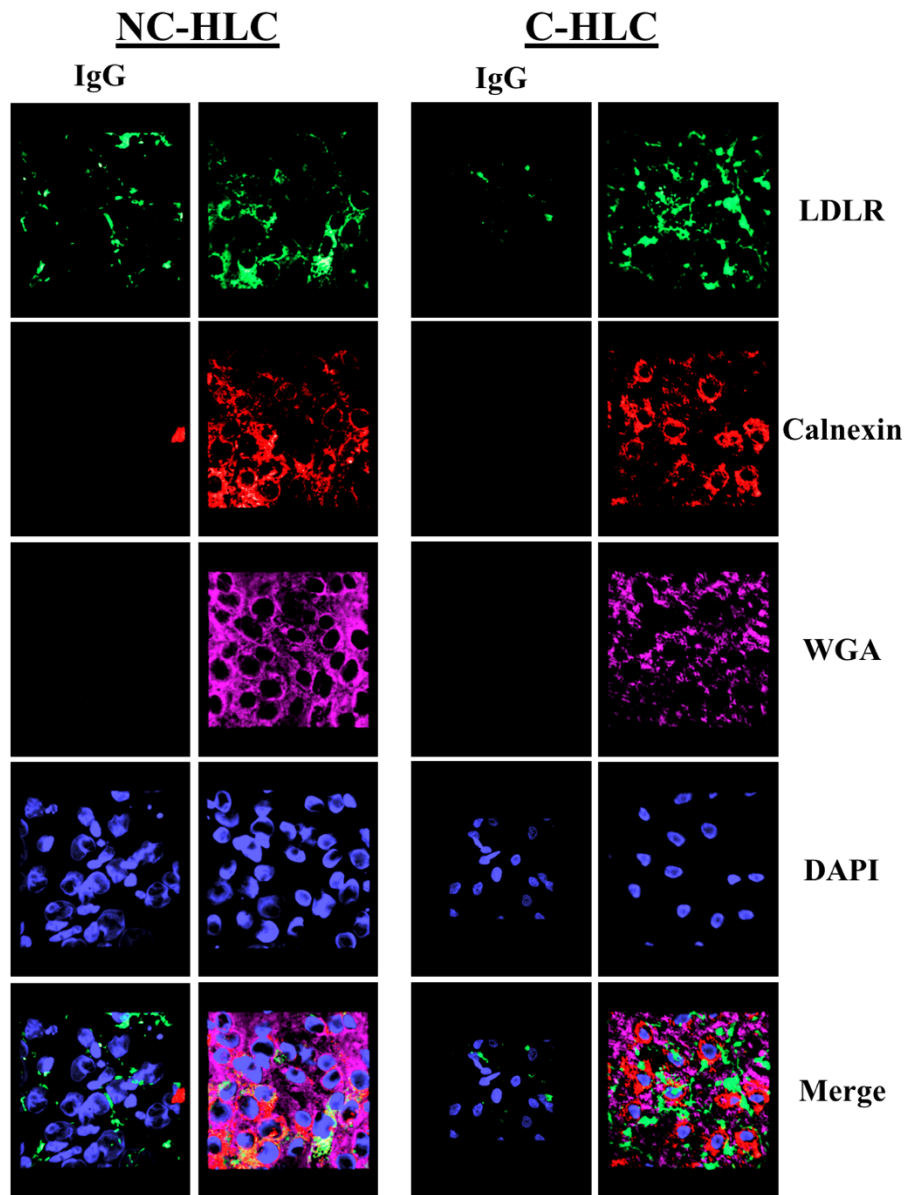


Figure 10a – Localization of the LDLR in corrected and non-corrected HLC

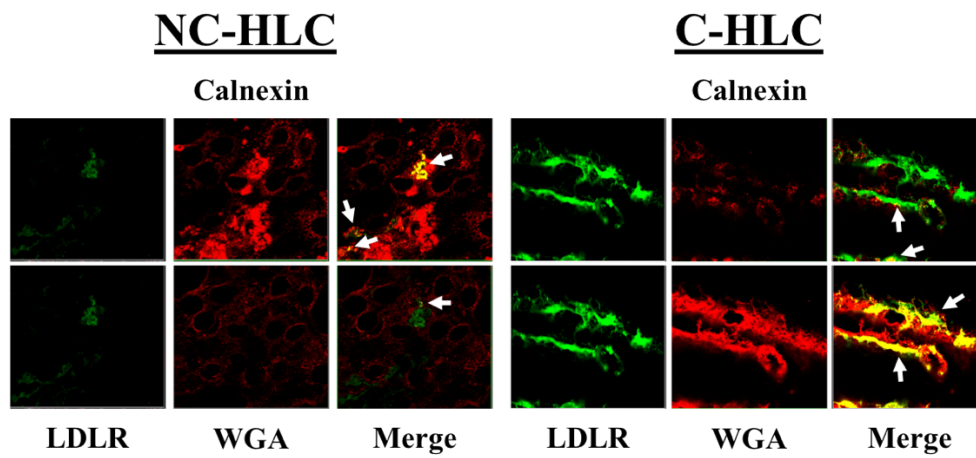


Figure 10b – Overlap of LDLR with calnexin or WGA in NC-HLC and C-HLC

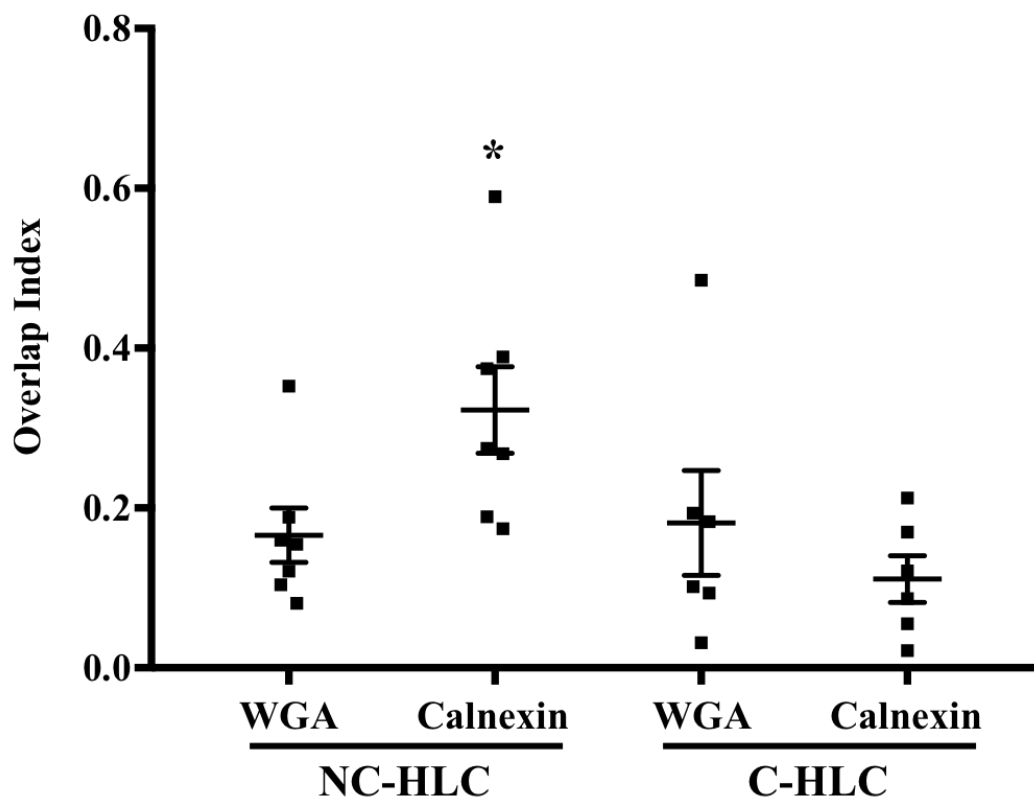


Figure 10c – Quantification of LDLR overlap with calnexin or WGA in NC-HLC and C-HLC

C. Recovery of Predominantly Mature LDLR Protein Expression Restores Cholesterol

Internalization in HLC

Upon confirming the predominant expression of the mature LDL receptor in the corrected cells, internalization of cholesterol was analyzed to determine if this was also mediated in the process. Cholesterol content was measured using the Thermo Fisher Amplex Red Cholesterol Assay Kit. HLC were treated with Rosuvastatin for 48 hours before methyl- β -cyclodextrin was added to remove any stored cholesterol (Francis et al., 1999). Cells were then incubated in LDL for six and 24 hours and analyzed via western blot. **Figure 11** shows a significant increase in cholesterol internalization overtime in the corrected cells, but little to no change in internalization is present in the non-corrected cells.

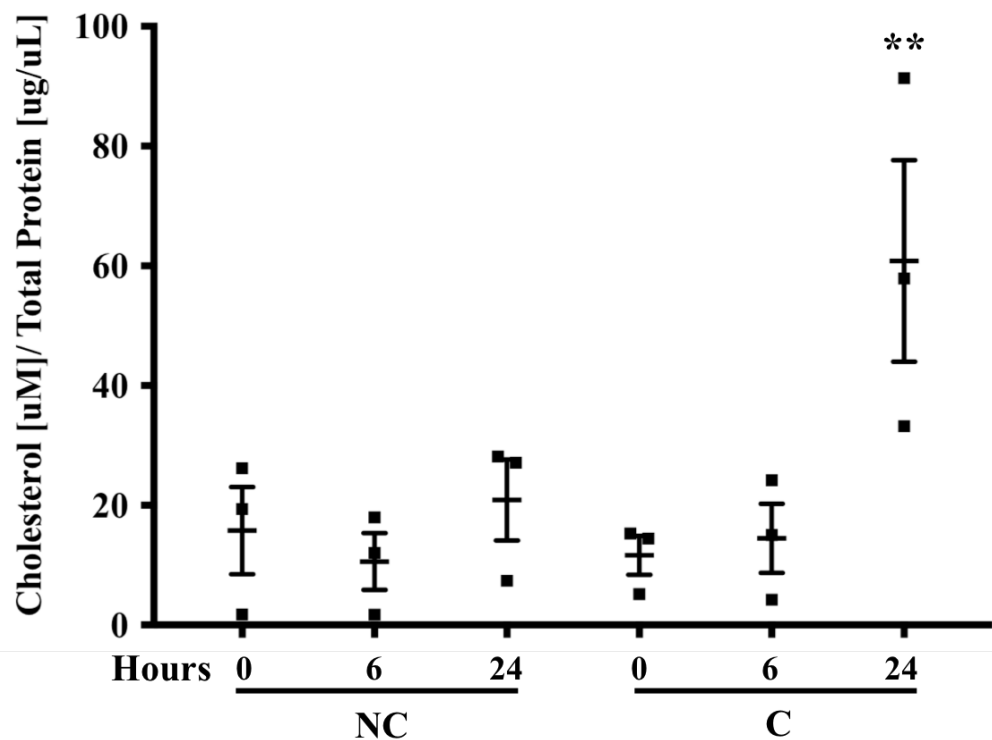


Figure 11 – Cholesterol internalization in non-corrected and corrected HLC over 0, 6, and 24 hours.

To further confirm the increase in cholesterol concentration overtime was a result of the exogenously-introduced cholesterol, rather than the remnants of any endogenously-produced cholesterol, cells were treated with DiI-LDL and imaged. Results shown in **Figure 12** further corroborate what was observed in the cells analyzed with the Amplex Kit. The corrected HLC display an internalization of DiI-LDL that increases with time from zero to 24 hours. In contrast, there is little internalization seen even at 24 hours in the non-corrected cells.

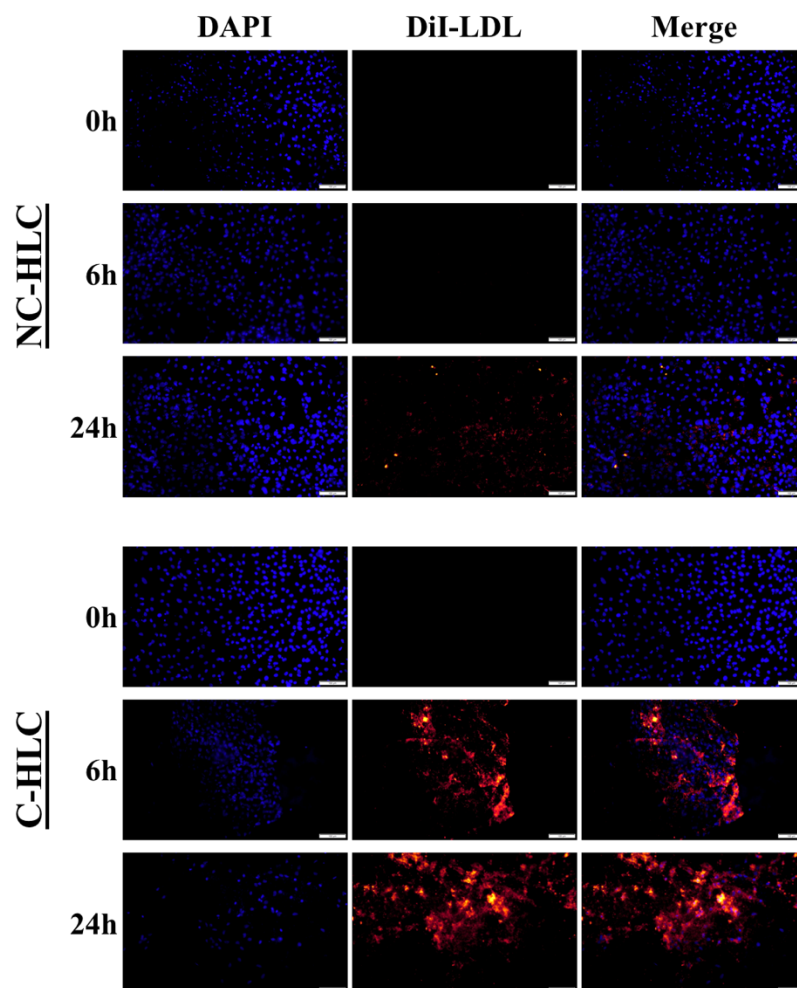


Figure 12 – DiI-LDL internalization in non-corrected and corrected HLC over 0, 6, and 24 hours.

D. HMG-CoA Reductase Activity in HLC

Next, HMG-CoA activity was determined using HPLC MS/MS. HMG-CoA Reductase catalyzes the reaction from HMG-CoA to Mevalonic Acid which equilibrates with the lactone form, Mevalonic lactone (MVL) at equilibrium (Kuzaj et al., 2014). Non-corrected and corrected HLC were treated with LPDS overnight before LDL in LPDS was added for a 24 hour treatment. Samples were prepared and analyzed used HPLC MS/MS along with protein samples collected for HMG-CoA protein expression. Mevalonic acid formation is one of the steps required in cholesterol synthesis, a process we would expect to be reduced in the corrected cells when they are able to obtain cholesterol from an exogenous source by using functional LDL receptors. We would, as a result, expect the concentration of MVL to decrease in the corrected cells, after the addition of LDL to the cell culture media, and the MVL concentration to stay the same in the non-corrected cells. **Figure 13a** shows no significant differences between cell lines in HMG-CoA Reductase activity. **Figure 13b** also shows no significant differences between cell lines in HMG-CoA Reductase protein expression.

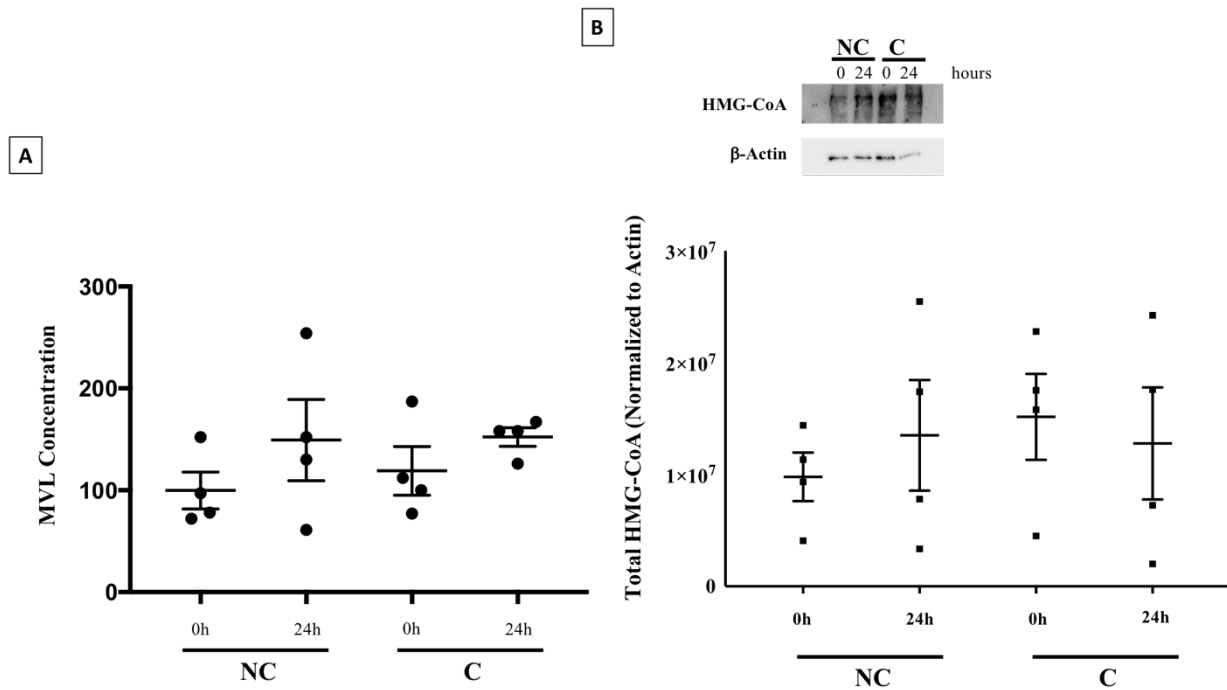


Figure 13 – (A) HMG-CoA Reductase enzymatic activity in non-corrected and corrected HLC as represented by the concentration of Mevalonic acid (MVL). (B) HMG-CoA Reductase protein expression in non-corrected and corrected HLC.

E. Accumulation of LDLR in the ER Does Not Upregulate ER Stress Markers

Lastly, ER stress markers were analyzed to determine if the accumulation of the immature LDLR in non-corrected HLC induced the unfolded protein response, as has been suggested by other publications characterizing this disease (Jorgensen et al., 2000; Sorensen, Ranheim, Bakken, Leren, & Kulseth, 2006). Non-corrected, corrected, and H1 iPSC and HLC were treated with Rosuvastatin, excess sterols, or tunicamycin in LPDS and collected for protein expression and transcript level evaluation. Tunicamycin upregulates BiP expression, an early marker of ER stress, and was used as a positive control to verify that the UPR is inducible in all of our cells. BiP and spliced XBP1 expression was analyzed. **Figure 14a** and **14b** show no

significant difference in BiP expression in neither iPSC or HLC. The significance displayed in the figure represent a difference between the treatments within each cell line, but not across the cell lines.

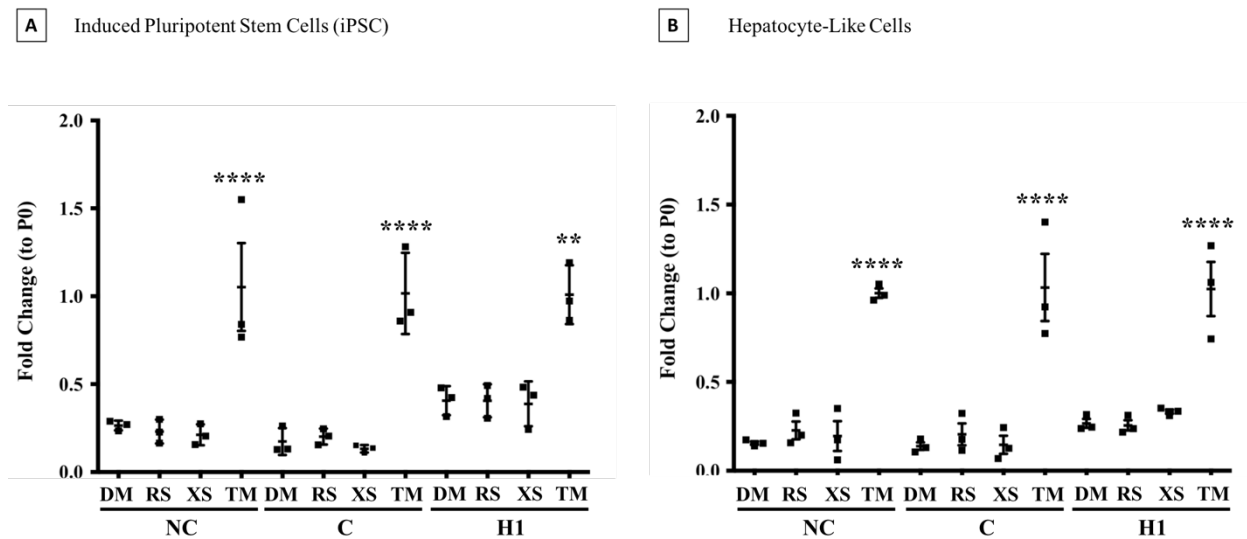


Figure 14 – BiP expression in (A) iPSC and (B) HLC treated with DMSO (DM), Rosuvastatin (RS), excess sterols (XS), or tunicamycin (TM). * $p < 0.05$, ** $p < 0.01$, *** $p < 0.001$.

XBPI is activated when unfolded proteins accumulate in the ER. IRE1 removes a 26-nucleotide intron from unspliced XBPI mRNA and leads to the production of a spliced product. **Figure 15a** and **15b** show no significant differences between spliced XBPI levels across cell lines. Splicing is upregulated in response to tunicamycin treatment within each cell line, but not across cell lines. We did observe upregulation in XBPI splicing in H1 HLC in all treatments that was not present in the NC- or C-HLC. This difference may be due to cell type, the NC- and C-HLC having differentiated from iPSC whereas the H1-HLC were differentiated from ESC. ER stress and the UPR is not the same in all stem cells and requires further investigation to

determine differences that may be present between different types of stem cells (Yang, Cheung, Tu, Miu, & Chan, 2016).

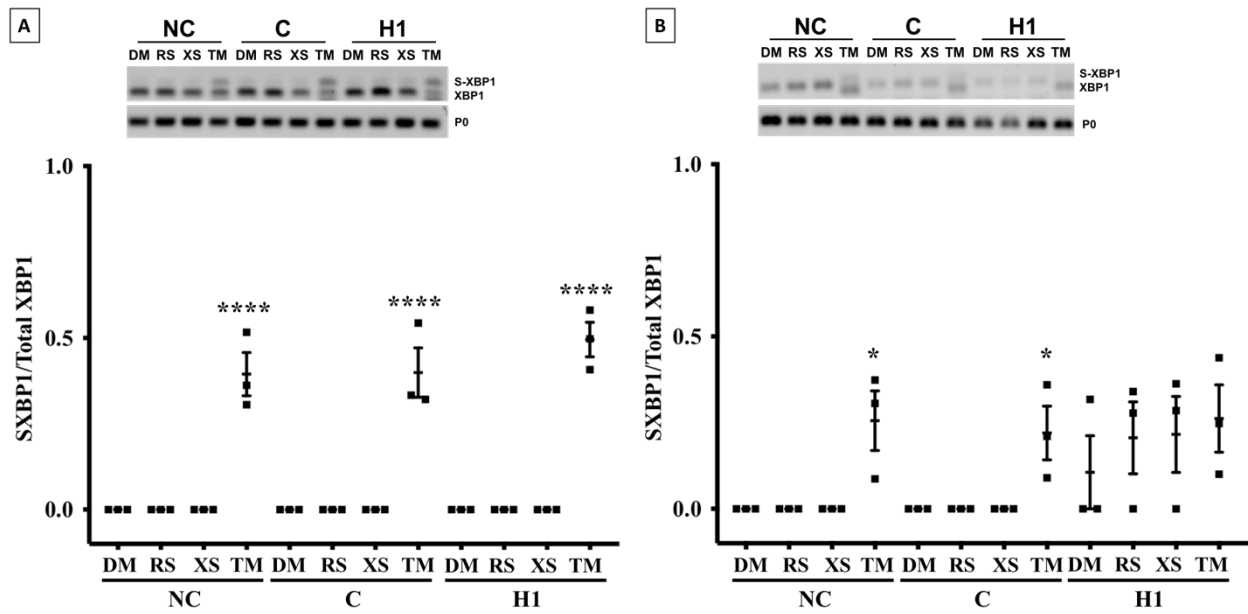


Figure 15 – Spliced XBP1 in (A) iPSC and (B) HLC treated with DMSO (DM), Rosuvastatin (RS), excess sterols (XS), or tunicamycin (TM). * $p < 0.05$, ** $p < 0.01$, *** $p < 0.001$.

IV. CONCLUSION

We observed an increase in the immature LDLR in NC cells that was mediated by CRISPR correction. This marked increase in the immature LDLR was not the result of increased regulation at the transcriptional level as we showed in our study. One point to consider here is how PCSK9 regulation plays a role and whether this would indeed affect LDLR at the transcriptional level. We did not look at PCSK9, but it would be important to determine if it is upregulated as a result of the statin treatment as has been suggested by the literature. From our results, we can presume that while PCSK9 may be upregulated, it is not upregulated in a significant manner that further compounds the expression of the LDL receptor. If PCSK9 was upregulated in a significant manner, then we can assume that it would degrade the small amount of functional LDL receptors present in NC cells and this would correlate with increases in LDLR at the transcriptional level, an increase that we did not observe.

We showed a co-localization of the LDLR with the ER in non-corrected HLC that was not seen in the corrected HLC, where the LDLR co-localized instead with the cell membrane. We saw significantly greater LDLR overlap with ER resident, calnexin, when compared to LDLR overlap with the plasma membrane further confirming the retention of the LDLR in the ER in the mutated cells and the mediation of this through CRISPR correction. This corrected co-localization was also further corroborated with our cholesterol internalization assays showing increased internalization with time with the corrected HLC whereas minimal cholesterol was internalized in the non-corrected HLC, expressing very little mature LDL receptor. The small amount of internalized cholesterol observed may represent non-receptor mediated pathways of cholesterol internalization, such as pinocytosis, in addition to the receptor-mediated pathway resulting from the few functional, mature LDL receptors.

Regulation of the LDL receptor is dependent on the careful balance that exists between the two sources of cholesterol, de novo synthesis and receptor-mediated endocytosis. We believed that HMG-CoA reductase activity would decrease in corrected HLC after the addition of LDL-C as a way of homeostatic feedback. The logic being, if cells were starved of exogenous cholesterol by culturing in lipoprotein deficient serum media, HMG-CoA reductase activity would increase to synthesize endogenous cholesterol. Then upon addition of exogenous LDL-C, HMG-CoA reductase activity would decrease to balance out the amount of endogenously-produced cholesterol and the cholesterol taken up through the receptors and that this decrease would not be observed in the non-corrected cells, due to low numbers of functional LDLR. This is not what we observed in our study and this represents a limitation here. In both corrected and non-corrected HLC, HMG-CoA reductase activity slightly, but not significantly, increase upon addition of LDL-C into the culture media. This leads us to question if our experimental conditions were appropriate for this analysis. Soufi et al. described the use of LPDS as physiologically irrelevant due to this abnormal upregulation of cholesterol metabolism genes by LPDS (Soufi, Ruppert, Kurt, & Schaefer, 2012). The entire duration of the treatment was conducted with LPDS media, both during starving the cell of exogenous cholesterol and introducing exogenous cholesterol. Soufi's finding suggests that because of LPDS's ability to upregulate cholesterol metabolism genes, they are upregulated to a magnitude that is not significantly affected by the addition of exogenous cholesterol. So perhaps, our experiment was a little counterintuitive in nature as we were upregulating cholesterol metabolism genes throughout the duration of the treatment, which is not physiologically representative, and in turn we were not able to see the true activity of HMG-CoA reductase as a regulatory portion of cholesterol homeostasis. To verify this, we can conduct a quick experiment to determine the effects of the

LPDS by culturing cells in basal media or basal media supplemented with LPDS and collect for mRNA or protein expression of cholesterol metabolism genes. Moving forward, it would be important to consider this experiment with some minor changes. One mainly being the duration of the treatment being conducted in a media that starves cells of exogenous cholesterol without simultaneously upregulating cholesterol metabolism genes. We could use a culture medium that doesn't necessarily starve cells of exogenous cholesterol and add exogenous LDL-C overtime and measure HMG-CoA reductase activity that way.

The unfolded protein response is activated as a result of protein accumulation in the ER. Publications have shown that proteins associated with the UPR are upregulated in Class II LDLR mutants (Jorgensen et al., 2000; Sorensen et al., 2006). Upon seeing expression of the immature LDLR in non-corrected iPSC and HLC and the co-localization of the LDLR with the ER in non-corrected HLC, we looked to see if this induced ER stress and activated the UPR. Our findings show that ER stress markers, BiP and spliced XBP1, are not upregulated in statin-treated non-corrected iPSC or HLC despite predominant expression of the immature LDLR. One thing to note is the conditions of the experiments performed in the publications that did report ER stress in Class II LDLR mutant cells. In Sorenson et al., cells were transfected with a constitutively-expressing mutant which may have resulted in levels of accumulation and in turn upregulated levels of ER markers many folds higher than what would occur in a true physiological environment. By using patient-derived mutant cells, we present a response that is more likely to be true in a physiological environment, but we cannot conclude that no ER stress is occurring. There still remain two other pathways and a number of proteins that we did not look at that need consideration before any such conclusion can be made. In the future, it is important to look at the

remaining two pathways, PERK and ATF6, and downstream proteins to provide a better overall picture of what is happening in the ER as a result of the protein accumulation.

V. FUTURE WORK

A. Bioartificial Liver

There remains a significant shortage of available livers to provide a cure for those suffering from FH. In addition, organ allocation protocols, cost of organ transplant, and rejection of donated organs present an additional obstacle further impeding FH patients from what may be their only real cure. Here, we have presented the feasibility of not only correcting mutant FH cells, but differentiating them into hepatocyte-like cells with restored cholesterol homeostasis that can be utilized in a number of applications. One such application may be the use of these corrected HLC in a decellularized liver matrix that can be isolated from the FH patients themselves or from organ donors with diseased livers that retain a functional matrix. Ott et al. presented the methodology for perfusing a decellularized heart matrix with neonatal cardiac cells in 2008 (Ott et al., 2008). The extracellular matrix (ECM) supplies cells with growth factors and signals that promote proliferation, regeneration, and organization of cells that is lacking *in vitro*. Of course there remain a number of steps before this can be fully executed. In Ott et al. only one injection site was used to perfuse the matrix with cardiac cells which resulted in only 2% pump function. This can be potentially mediated by introducing multiple injection sites to provide a more widespread perfusion of cells. For the liver specifically, it is also important to introduce non-parenchymal cells in order to provide the organ with all necessary cell types to perform the many functions of the liver. These cells may include sinusoidal endothelial cells, Kupffer cells, and hepatic stellate cells (Kmiec, 2001). This application would give use to livers that may not be functional or healthy enough to be transplanted due to presence of disease or other damage, but retain a functional ECM that provides a physiologically-derived blank canvas that can be put to use. Another benefit of this application is the use of autologous cells in order to reduce possibility of rejection. As we have

presented in this work, patient-derived cells would be isolated, corrected, and differentiated into mature hepatocytes before perfusion into a donated liver matrix.

B. Use in Personalized Drug Therapy

iPSC present an attractive and physiologically relevant method for developing new drugs and evaluating cytotoxicity. In addition, patient-derived iPSC provide a more intimate overview of the disease affecting each patient, specifically. Often, FH patients are prescribed a combination treatment protocol consisting of lifestyle changes, statin therapy, and lipoprotein apheresis. Regardless of similarity in the disease, patient response to treatments differ. HoFH patient-derived iPSC can be differentiated into HLC and used to test different combinations of treatment protocols. For example, there exist a wide range of statin drugs so testing the efficacy of each one on patient-derived cells can provide a more rapid and efficient method for determining the optimal drug and dose specific to that patient. This saves time and provides optimal treatment for the patient quicker than monitoring cholesterol levels in relation to each attempted drug protocol.

APPENDIX

1. Antibodies and Fluorophores

Antigen	Host	Dilution	Distributor
LDLR	Goat	1:100 (ICC), 1:1000 (WB)	R&D Systems, Minneapolis, MN
Calnexin	Mouse	1:100	EMD Millipore, Billerica, MA
Biotinylated-Wheat Germ Agglutinin		1:200	Vector Laboratories, Burlingame, CA
β -Actin	Mouse	1:1000	Santa Cruz Biotechnology, Dallas, TX
gIgG	Goat	1:100	Novus Biologicals, Littleton, CO
mIgG2b	Mouse	1:1000	Invitrogen, Carlsbad, CA
Alexa Fluor Donkey Anti-Goat 488 nm		1:1000	Invitrogen
Alexa Fluor Donkey Anti-Mouse 546 nm		1:1000	Invitrogen
Streptavidin-649		1:1000	Vector Laboratories
HRP-Bovine Anti-Goat IgG H+L		1:5000	Jackson ImmunoResearch, West Grove, PA
Anti-Mouse IgG, HRP-linked		1:5000	Cell Signaling, Danvers, MA

2. Primers for qPCR/PCR

Gene	Primer 1 (5' → 3')	Primer 2 (5' → 3')	Product Size (bp)
LDLR	GCAGTGTGACCGGGAATATGA	GTTGGTCCCGCACTCTTTGA	115
BiP	CCGTTCAAGGTGGTTGAAAAGAA	TGGCGTTGGGCATCATTAATA	200
(S) XBP1	CCTGGTTGCTGAAGAGGAGG	GGCAGGCTGCTGTCCTCAT	150 ; 124
P0	TCGACAATGGCAGCATCTAC	ATCCGTCTCCACAGACAAGG	200

REFERENCES

- Ajufo, E., & Cuchel, M. (2016). Recent Developments in Gene Therapy for Homozygous Familial Hypercholesterolemia. *Curr Atheroscler Rep*, 18(5), 22. doi:10.1007/s11883-016-0579-0
- Akiyamen, L. E., Genest, J., Shan, S. D., Reel, R. L., Albaum, J. M., Chu, A., & Tu, J. V. (2017). Estimating the prevalence of heterozygous familial hypercholesterolaemia: a systematic review and meta-analysis. *BMJ Open*, 7(9), e016461. doi:10.1136/bmjopen-2017-016461
- Benn, M., Nordestgaard, B. G., Grande, P., Schnohr, P., & Tybjaerg-Hansen, A. (2010). PCSK9 R46L, low-density lipoprotein cholesterol levels, and risk of ischemic heart disease: 3 independent studies and meta-analyses. *J Am Coll Cardiol*, 55(25), 2833-2842. doi:10.1016/j.jacc.2010.02.044
- Bhatia, S. N., Underhill, G. H., Zaret, K. S., & Fox, I. J. (2014). Cell and tissue engineering for liver disease. *Sci Transl Med*, 6(245), 245sr242. doi:10.1126/scitranslmed.3005975
- Bouhairie, V. E., & Goldberg, A. C. (2015). Familial hypercholesterolemia. *Cardiol Clin*, 33(2), 169-179. doi:10.1016/j.ccl.2015.01.001
- Brown, M. S., & Goldstein, J. L. (1979). Receptor-mediated endocytosis: insights from the lipoprotein receptor system. *Proc Natl Acad Sci U S A*, 76(7), 3330-3337.
- Brown, M. S., & Goldstein, J. L. (1986). A receptor-mediated pathway for cholesterol homeostasis. *Science*, 232(4746), 34-47.
- Buja, L. M., Kovanen, P. T., & Bilheimer, D. W. (1979). Cellular pathology of homozygous familial hypercholesterolemia. *Am J Pathol*, 97(2), 327-357.
- Burns, F. S. (1920). A contribution to the study of the etiology of xanthoma multiplex. *Archives of Dermatology and Syphilology*, 2(4), 415-429. doi:10.1001/archderm.1920.02350100003001
- Calnexin, calreticulin and the folding of glycoproteins. (1997). *Trends in Cell Biology*, 7(5), 193-200. doi:[https://doi.org/10.1016/S0962-8924\(97\)01032-5](https://doi.org/10.1016/S0962-8924(97)01032-5)
- Cerqueira, N. M., Oliveira, E. F., Gesto, D. S., Santos-Martins, D., Moreira, C., Moorthy, H. N., . . . Fernandes, P. A. (2016). Cholesterol Biosynthesis: A Mechanistic Overview. *Biochemistry*, 55(39), 5483-5506. doi:10.1021/acs.biochem.6b00342
- Cortes, V. A., Busso, D., Maiz, A., Arteaga, A., Nervi, F., & Rigotti, A. (2014). Physiological and pathological implications of cholesterol. *Front Biosci (Landmark Ed)*, 19, 416-428.
- Crawford, A. R., Smith, A. J., Hatch, V. C., Oude Elferink, R. P., Borst, P., & Crawford, J. M. (1997). Hepatic secretion of phospholipid vesicles in the mouse critically depends on mdr2 or MDR3 P-glycoprotein expression. Visualization by electron microscopy. *J Clin Invest*, 100(10), 2562-2567. doi:10.1172/jci119799
- Cuchel, M., Bruckert, E., Ginsberg, H. N., Raal, F. J., Santos, R. D., Hegele, R. A., . . . Chapman, M. J. (2014). Homozygous familial hypercholesterolaemia: new insights and guidance for clinicians to improve detection and clinical management. A position paper from the Consensus Panel on Familial Hypercholesterolaemia of the European Atherosclerosis Society. *Eur Heart J*, 35(32), 2146-2157. doi:10.1093/eurheartj/ehu274
- Culme-Seymour, E. J., Davie, N. L., Brindley, D. A., Edwards-Parton, S., & Mason, C. (2012). A decade of cell therapy clinical trials (2000-2010). *Regen Med*, 7(4), 455-462. doi:10.2217/rme.12.45

- Dash, S., Xiao, C., Morgantini, C., & Lewis, G. F. (2015). New Insights into the Regulation of Chylomicron Production. *Annu Rev Nutr*, 35, 265-294. doi:10.1146/annurev-nutr-071714-034338
- Dawson, P. A., & Rudel, L. L. (1999). Intestinal cholesterol absorption. *Curr Opin Lipidol*, 10(4), 315-320.
- de Ferranti, S. D., Rodday, A. M., Mendelson, M. M., Wong, J. B., Leslie, L. K., & Sheldrick, R. C. (2016). Prevalence of Familial Hypercholesterolemia in the 1999 to 2012 United States National Health and Nutrition Examination Surveys (NHANES). *Circulation*, 133(11), 1067-1072. doi:10.1161/circulationaha.115.018791
- Ellgaard, L., & Helenius, A. (2003). Quality control in the endoplasmic reticulum. *Nat Rev Mol Cell Biol*, 4(3), 181-191. doi:10.1038/nrm1052
- Fischbach, M. A., Bluestone, J. A., & Lim, W. A. (2013). Cell-based therapeutics: the next pillar of medicine. *Sci Transl Med*, 5(179), 179ps177. doi:10.1126/scitranslmed.3005568
- Fra, A. M., Fagioli, C., Finazzi, D., Sitia, R., & Alberini, C. M. (1993). Quality control of ER synthesized proteins: an exposed thiol group as a three-way switch mediating assembly, retention and degradation. *Embo j*, 12(12), 4755-4761.
- Francis, S. A., Kelly, J. M., McCormack, J., Rogers, R. A., Lai, J., Schneeberger, E. E., & Lynch, R. D. (1999). Rapid reduction of MDCK cell cholesterol by methyl-beta-cyclodextrin alters steady state transepithelial electrical resistance. *Eur J Cell Biol*, 78(7), 473-484.
- Goldstein, J. L., & Brown, M. S. (2001). Molecular medicine. The cholesterol quartet. *Science*, 292(5520), 1310-1312.
- Grossman, M., Rader, D. J., Muller, D. W., Kolansky, D. M., Kozarsky, K., Clark, B. J., 3rd, . . . et al. (1995). A pilot study of ex vivo gene therapy for homozygous familial hypercholesterolaemia. *Nat Med*, 1(11), 1148-1154.
- Guha, P., Morgan, J. W., Mostoslavsky, G., Rodrigues, N. P., & Boyd, A. S. (2013). Lack of immune response to differentiated cells derived from syngeneic induced pluripotent stem cells. *Cell Stem Cell*, 12(4), 407-412. doi:10.1016/j.stem.2013.01.006
- H H Hobbs, D W Russell, M S Brown, a., & Goldstein, J. L. (1990). The LDL Receptor Locus in Familial Hypercholesterolemia: Mutational Analysis of a Membrane Protein. *Annual Review of Genetics*, 24(1), 133-170. doi:10.1146/annurev.ge.24.120190.001025
- Harada-Shiba, M., Arai, H., Ishigaki, Y., Ishibashi, S., Okamura, T., Ogura, M., . . . Yokote, K. (2018). Guidelines for Diagnosis and Treatment of Familial Hypercholesterolemia 2017. *J Atheroscler Thromb*, 25(8), 751-770. doi:10.5551/jat.CR003
- Harada-Shiba, M., Tajima, S., Yokoyama, S., Miyake, Y., Kojima, S., Tsushima, M., . . . Yamamoto, A. (1992). Siblings with normal LDL receptor activity and severe hypercholesterolemia. *Arterioscler Thromb*, 12(9), 1071-1078.
- Hay, D. C., Fletcher, J., Payne, C., Terrace, J. D., Gallagher, R. C., Snoeys, J., . . . Iredale, J. P. (2008). Highly efficient differentiation of hESCs to functional hepatic endoderm requires ActivinA and Wnt3a signaling. *Proc Natl Acad Sci U S A*, 105(34), 12301-12306. doi:10.1073/pnas.0806522105
- Hay, D. C., Zhao, D., Fletcher, J., Hewitt, Z. A., McLean, D., Urruticoechea-Uriguen, A., . . . Cui, W. (2008). Efficient differentiation of hepatocytes from human embryonic stem cells exhibiting markers recapitulating liver development in vivo. *Stem Cells*, 26(4), 894-902. doi:10.1634/stemcells.2007-0718

- Hellman, R., Vanhove, M., Lejeune, A., Stevens, F. J., & Hendershot, L. M. (1999). The in vivo association of BiP with newly synthesized proteins is dependent on the rate and stability of folding and not simply on the presence of sequences that can bind to BiP. *J Cell Biol*, *144*(1), 21-30.
- Hopkins, P. N., Toth, P. P., Ballantyne, C. M., & Rader, D. J. (2011). Familial hypercholesterolemias: prevalence, genetics, diagnosis and screening recommendations from the National Lipid Association Expert Panel on Familial Hypercholesterolemia. *J Clin Lipidol*, *5*(3 Suppl), S9-17. doi:10.1016/j.jacl.2011.03.452
- Insull, W., Jr. (2006). Clinical utility of bile acid sequestrants in the treatment of dyslipidemia: a scientific review. *South Med J*, *99*(3), 257-273. doi:10.1097/01.smj.0000208120.73327.db
- Jain, A., Jain, K., Kesharwani, P., & Jain, N. K. (2013). Low density lipoproteins mediated nanoplatfoms for cancer targeting. *Journal of Nanoparticle Research*, *15*(9), 1888. doi:10.1007/s11051-013-1888-7
- Jorgensen, M. M., Jensen, O. N., Holst, H. U., Hansen, J. J., Corydon, T. J., Bross, P., . . . Gregersen, N. (2000). Grp78 is involved in retention of mutant low density lipoprotein receptor protein in the endoplasmic reticulum. *J Biol Chem*, *275*(43), 33861-33868. doi:10.1074/jbc.M004663200
- Kaufman, R. J. (2004). Regulation of mRNA translation by protein folding in the endoplasmic reticulum. *Trends Biochem Sci*, *29*(3), 152-158. doi:10.1016/j.tibs.2004.01.004
- Keele, K. D. (1951). Leonardo da Vinci, and the movement of the heart. *Proc R Soc Med*, *44*(3), 209-213.
- Khachadurian, A. K. (1964). THE INHERITANCE OF ESSENTIAL FAMILIAL HYPERCHOLESTEROLEMIA. *Am J Med*, *37*, 402-407.
- Kmiec, Z. (2001). Cooperation of liver cells in health and disease. *Adv Anat Embryol Cell Biol*, *161*, Iii-xiii, 1-151.
- Kusters, D. M., Hommsma, S. J., Hutten, B. A., Twickler, M. T., Avis, H. J., van der Post, J. A., & Stroes, E. S. (2010). Dilemmas in treatment of women with familial hypercholesterolaemia during pregnancy. *Neth J Med*, *68*(1), 299-303.
- Kuzaj, P., Kuhn, J., Faust, I., Knabbe, C., & Hendig, D. (2014). Measurement of HMG CoA reductase activity in different human cell lines by ultra-performance liquid chromatography tandem mass spectrometry. *Biochem Biophys Res Commun*, *443*(2), 641-645. doi:10.1016/j.bbrc.2013.12.013
- Lagor, W. R., & Millar, J. S. (2009). Overview of the LDL receptor: relevance to cholesterol metabolism and future approaches for the treatment of coronary heart disease. *Journal of Receptor, Ligand and Channel Research*, *3*, 14. doi:<https://doi.org/10.2147/JRLCR.S6033>
- Lambert, G., Chatelais, M., Petrides, F., Passard, M., Thedrez, A., Rye, K. A., . . . Marais, A. D. (2014). Normalization of low-density lipoprotein receptor expression in receptor defective homozygous familial hypercholesterolemia by inhibition of PCSK9 with alirocumab. *J Am Coll Cardiol*, *64*(21), 2299-2300. doi:10.1016/j.jacc.2014.07.995
- Lu, K., Lee, M. H., & Patel, S. B. (2001). Dietary cholesterol absorption; more than just bile. *Trends Endocrinol Metab*, *12*(7), 314-320.
- Müller, C. (1939). Angina pectoris in hereditary xanthomatosis. *Archives of Internal Medicine*, *64*(4), 675-700. doi:10.1001/archinte.1939.00190040016002

- Myant, N. B. (1993). Familial defective apolipoprotein B-100: a review, including some comparisons with familial hypercholesterolaemia. *Atherosclerosis*, *104*(1-2), 1-18.
- Nicolas, C. T., Wang, Y., & Nyberg, S. L. (2016). Cell therapy in chronic liver disease. *Curr Opin Gastroenterol*, *32*(3), 189-194. doi:10.1097/mog.0000000000000262
- Nordestgaard, B. G., Chapman, M. J., Humphries, S. E., Ginsberg, H. N., Masana, L., Descamps, O. S., . . . Tybjaerg-Hansen, A. (2013). Familial hypercholesterolaemia is underdiagnosed and undertreated in the general population: guidance for clinicians to prevent coronary heart disease: consensus statement of the European Atherosclerosis Society. *Eur Heart J*, *34*(45), 3478-3490a. doi:10.1093/eurheartj/eh273
- Ogura, M. (2018). PCSK9 inhibition in the management of familial hypercholesterolemia. *J Cardiol*, *71*(1), 1-7. doi:10.1016/j.jjcc.2017.07.002
- Omer, L., Hudson, E. A., Zheng, S., Hoying, J. B., Shan, Y., & Boyd, N. L. (2017). CRISPR Correction of a Homozygous Low-Density Lipoprotein Receptor Mutation in Familial Hypercholesterolemia Induced Pluripotent Stem Cells. *HepatoL Commun*, *1*(9), 886-898. doi:10.1002/hep4.1110
- Ose, L. (2008). The real code of leonardo da vinci. *Curr Cardiol Rev*, *4*(1), 60-62. doi:10.2174/157340308783565401
- Ott, H. C., Matthiesen, T. S., Goh, S. K., Black, L. D., Kren, S. M., Netoff, T. I., & Taylor, D. A. (2008). Perfusion-decellularized matrix: using nature's platform to engineer a bioartificial heart. *Nat Med*, *14*(2), 213-221. doi:10.1038/nm1684
- Pan, X., & Hussain, M. M. (2012). Gut triglyceride production. *Biochim Biophys Acta*, *1821*(5), 727-735. doi:10.1016/j.bbali.2011.09.013
- Pejic, R. N. (2014). Familial hypercholesterolemia. *Ochsner J*, *14*(4), 669-672.
- Ramakrishnan, V. M., Yang, J. Y., Tien, K. T., McKinley, T. R., Bocard, B. R., Majjub, J. G., . . . Boyd, N. L. (2015). Restoration of Physiologically Responsive Low-Density Lipoprotein Receptor-Mediated Endocytosis in Genetically Deficient Induced Pluripotent Stem Cells. *Sci Rep*, *5*, 13231. doi:10.1038/srep13231
- Ron, D., & Walter, P. (2007). Signal integration in the endoplasmic reticulum unfolded protein response. *Nat Rev Mol Cell Biol*, *8*(7), 519-529. doi:10.1038/nrm2199
- Schindler, A. J., & Schekman, R. (2009). In vitro reconstitution of ER-stress induced ATF6 transport in COPII vesicles. *Proc Natl Acad Sci U S A*, *106*(42), 17775-17780. doi:10.1073/pnas.0910342106
- Sharifi, M., Futema, M., Nair, D., & Humphries, S. E. (2017). Genetic Architecture of Familial Hypercholesterolaemia. *Curr Cardiol Rep*, *19*(5), 44. doi:10.1007/s11886-017-0848-8
- Singh, S., & Bittner, V. (2015). Familial hypercholesterolemia--epidemiology, diagnosis, and screening. *Curr Atheroscler Rep*, *17*(2), 482. doi:10.1007/s11883-014-0482-5
- Singh, V. K., Kalsan, M., Kumar, N., Saini, A., & Chandra, R. (2015). Induced pluripotent stem cells: applications in regenerative medicine, disease modeling, and drug discovery. *Front Cell Dev Biol*, *3*, 2. doi:10.3389/fcell.2015.00002
- Sjouke, B., Kusters, D. M., Kindt, I., Besseling, J., Defesche, J. C., Sijbrands, E. J., . . . Hovingh, G. K. (2015). Homozygous autosomal dominant hypercholesterolaemia in the Netherlands: prevalence, genotype-phenotype relationship, and clinical outcome. *Eur Heart J*, *36*(9), 560-565. doi:10.1093/eurheartj/ehu058
- Sorensen, S., Ranheim, T., Bakken, K. S., Leren, T. P., & Kulseth, M. A. (2006). Retention of mutant low density lipoprotein receptor in endoplasmic reticulum (ER) leads to ER stress. *J Biol Chem*, *281*(1), 468-476. doi:10.1074/jbc.M507071200

- Soufi, M., Ruppert, V., Kurt, B., & Schaefer, J. R. (2012). The impact of severe LDL receptor mutations on SREBP-pathway regulation in homozygous familial hypercholesterolemia (FH). *Gene*, 499(1), 218-222. doi:10.1016/j.gene.2012.02.031
- Soutar, A. K., & Naoumova, R. P. (2007). Mechanisms of disease: genetic causes of familial hypercholesterolemia. *Nat Clin Pract Cardiovasc Med*, 4(4), 214-225. doi:10.1038/ncpcardio0836
- Staels, B., & Fonseca, V. A. (2009). Bile acids and metabolic regulation: mechanisms and clinical responses to bile acid sequestration. *Diabetes Care*, 32 Suppl 2, S237-245. doi:10.2337/dc09-S355
- Stein, E. A., Ose, L., Retterstol, K., Tonstad, S., Schleman, M., Harris, S., & Sager, P. (2007). Further reduction of low-density lipoprotein cholesterol and C-reactive protein with the addition of ezetimibe to maximum-dose rosuvastatin in patients with severe hypercholesterolemia. *J Clin Lipidol*, 1(4), 280-286. doi:10.1016/j.jacl.2007.07.003
- Takahashi, K., & Yamanaka, S. (2006). Induction of pluripotent stem cells from mouse embryonic and adult fibroblast cultures by defined factors. *Cell*, 126(4), 663-676. doi:10.1016/j.cell.2006.07.024
- Yang, Y., Cheung, H. H., Tu, J., Miu, K. K., & Chan, W. Y. (2016). New insights into the unfolded protein response in stem cells. *Oncotarget*, 7(33), 54010-54027. doi:10.18632/oncotarget.9833

VITA

Lubna Hindi

Louisville, KY 40241 | LubnaHindi04@gmail.com

Education

- Master of Engineering** in Bioengineering Dec 2018
J.B. Speed School of Engineering
Louisville, KY
- Bachelor of Science** in Bioengineering Dec 2017
J.B. Speed School of Engineering
Louisville, KY

Employment

- Family Education Teacher** Feb 2018 – Present
Americana World Community Center
- Student Assistant** Feb 2014 – Dec 2018
Dean's Office, University of Louisville J.B. Speed School of Engineering
- Student Co-Op** July 2016 – Aug 2017
ASNB Muscle Lab, University of Louisville School of Medicine
- Student Co-Op** Jan 2015 – May 2015
Bioimaging and Bioinstrumentation, Cardiovascular Innovation Institute
- Assistant News Editor** Jun 2014 – Dec 2014
The Louisville Cardinal

Activities

- Volunteer** 2016 – Present
Supplies Over Seas
- President** 2017
Biomedical Engineering Society
- President** 2016 – 2017
Sigma Alpha Lambda
- Vice President** 2015 – 2016
Sigma Alpha Lambda
- President** 2014 – 2016
Student Organization for Alumni Relations

Ex Officio Director

University of Louisville Alumni Association

2014 – 2016

Publications

- 1) **Hindi, L.**, McMillan, J. D., Afroze, D., Hindi, S. M. and Kumar, A. (2017). Isolation, Culturing, and Differentiation of Primary Myoblasts from Skeletal Muscle of Adult Mice. *Bio-protocol* 7(9): e2248
- 2) Hindi, S.M., Shin, J., Gallot, Y., Straught, A., Simionescu-Bankston, A., **Hindi, L.**, Xiong, G., Friedland, R. (2017). MyD88 promotes myoblast fusion in a cell-autonomous manner. *Nature Communications*